Synthesis Structures and Properties of Ruthenium Piano Stool Complexes

A Thesis submitted to The University of Manchester for the degree of MPhil of Philosophy in the Faculty of Science & Engineering

2016

Peng Yi

School of Chemistry

Contents

Total Word Count: 15253

List of Figures and Schemes

List of Tables

Abbreviations

1D	One dimension
2D	Two dimensions
BBO	β-BaB_2O_4
Bz	Benzene
Cymene or Cym	P-cymene (1-isopropyl-4-methylbenzene)
HMB	Hexamethylbenzene
Py	Pyridine
Pic	4-Picoline
Ein	Ethyl isonicotinate
Ppy	4-Phenylpyridine
D-π-A	Donor-π-Acceptor
DAST	(E)-4'-(dimethylamino)-N-methyl-4-stilbazolium tosylate
DAPSH	*Trans*-4′-(dimethylamino)-*N*-phenyl-4-stilbazolium hexafluorophosphate
HRS	Hyper-Rayleigh scattering
DFT	Density functional theory
ITO	Indium tin oxide
KDP	KH_2PO_4
KTP	$KTiOPO_4$
DMF	*N*,*N*-Dimethylformamide
DCM	Dichloromethane
DMSO	Dimethyl sulfoxide
CD_3CN	Trideuteroacetonitrile
CD_3SOCD_3	Dimethylsulfoxide-d_6
LB	Langmuir-Blodgett film
MLCT	Metal-to-ligand-charge-transfer
Mimid	N-methylimidazole

LMCT	Ligand-to-metal-charge-transfer
NLO	Nonlinear optical
NMR	Nuclear magnetic resonance
SHG	Second harmonic generation
SOS	Sum-over-state
UV-visible	Ultraviolet-visible
BPh_4	Tetraphenylborate
TGA	Thermogravimetric analysis
HOMO	Highest occupied molecular orbital

Abstract

This research investigated the synthesis of a series of new C_{3v} Ru^{II} complexes with pyridine or pyridyl ligands. Commercial ruthenium chloride dimers ($[Ru(Bz)Cl_2]_2$, $[Ru(Cym)Cl_2]_2$, $[Ru(HMB)Cl_2]_2$) were initially used to synthesise the important precursors $[Ru(Bz)(N_2H_4)_3][BPh_4]_2$ (**1**), $[Ru(Cym)(N_2H_4)_3][BPh_4]_2$ (**6**) and $[Ru(HMB)(N_2H_4)_3][BPh_4]_2$ (**12**), which was followed by the synthesis of a series of Ruthenium tris-pyridyl complexes that included $[Ru(Cym)(ein)_3][BPh_4]_2$ (**9**). Investigations into different purification methods, which included recrystallisation in different solvent combination systems, alumina column and sephadex column revealed that the most efficient method for a silica column was eluant DCM:acetone(dry)= 95:5 or DCM:acetonitrile (dry)= 95:5. A range of novel compounds was successfully made. Complexes $[Ru(Bz)(N_2H_4)_3][BPh_4]_2$ **(1**), $[Ru(Bz)(py)_3][BPh_4]_2$ (**2**), $[Ru(Cym)(N_2H_4)_3][BPh_4]_2$ (**6**), $[Ru(Cym)(py)_3][BPh_4]_2$ (**7**), $[Ru(Cym)(pic)_3][BPh_4]_2$ (**8**) were all known compounds. Compounds $[Ru(Bz)(pic)_3][BPh_4]_2$ (**3**), $[Ru(Bz)(ein)_3][BPh_4]_2$ (**4**), $[Ru(Bz)(ppy)_3][BPh_4]_2$ (**5**), $[Ru(Cym)(ein)_3][BPh_4]_2$ (**9**), $[Ru(Cym)(ppy)_3][BPh_4]_2$ (**10**), $[Ru(HMB)(N_2H_4)_3][BPh_4]_2$ (**12**), $[Ru(HMB)(py)_3][Cl]_2$ (**13**), $[Ru(HMB)(pic)_3][Cl]_2$ (**14**), $[Ru(HMB)(ein)_3][Cl]_2$ (**15**) and $[Ru(HMB)(ppy)_3][BPh_4]_2$ (**16**) are all new complexes. The compounds (**1-10)** were fully characterised by electronic spectroscopy and electrochemical methods. Eight crystal structures of $[Ru(Bz)(N_2H_4)_3][BPh_4]_2$ (**1**), $[Ru(Bz)(py)_3][BPh_4]_2$ (**2**), $[Ru(Cym)(N_2H_4)_3][BPh_4]_2$ (**6**), $[Ru(py)_3(DMF)_3][BPh_4]_2$ (**11**), $[Ru(HMB)(N_2H_4)_3][BPh_4]_2$ (**12**), $[Ru(HMB)(py)(Cl)_2]$ (**17**), $[Ru(HMB)(pic)(Cl)_2]$ (**18**) and $[Ru(HMB)(pic)(Cl)_2]\bullet CH_2Cl_2$ (**19**) were obtained as well.

Declaration

I hereby declare that no portion of the work referred to in the thesis has been submitted in support of an application for another degree or qualification of this or any other university or other institute of learning.

Copyright Statement

The author of this thesis (including any appendices and/or schedules to this thesis) owns certain copyright or related rights in it (the “Copyright”) and he has given The University of Manchester certain rights to use such Copyright, including for administrative purposes.

Copies of this thesis, either in full or in extracts and whether in hard or electronic copy, may be made **only** in accordance with the Copyright, Designs and Patents Act 1988 (as amended) and regulations issued under it or, where appropriate, in accordance with licensing agreements which the University has from time to time. This page must form part of any such copies made.

The ownership of certain Copyright, patents, designs, trademarks and other intellectual property (the “Intellectual Property”) and any reproductions of copyright works in the thesis, for example graphs and tables (“Reproductions”), which may be described in this thesis, may not be owned by the author and may be owned by third parties. Such Intellectual Property and Reproductions cannot and must not be made available for use without the prior written permission of the owner(s) of the relevant Intellectual Property and/or Reproductions.

Further information on the conditions under which disclosure, publication and commercialisation of this thesis, the Copyright and any Intellectual Property and/or

Reproductions described in it may take place is available in the University IP Policy (see http://documents.manchester.ac.uk/DocuInfo.aspx?DocID=487), in any relevant Thesis restriction declarations deposited in the University Library, The University Library's regulations (see http://www.manchester.ac.uk/library/aboutus/regulations) and in The University's policy on Presentation of Theses.

Acknowledgements

Firstly, I want to give big thanks to my supervisor Ben Coe for these years teaching and guiding. I will not forget the support and the smile on his face in my life. The logical approach of doing things he taught me will have a huge impact during my life.

Secondly, I also want to say thanks to Mark Whiteley and Robin Pritchard. They helped me quite a lot since I have been in this university. And huge thanks for Alan Brisdon, David Collison, James Raftery, all the technical staff at the University of Manchester. I would like to say thanks to all the people in our group including Rachel, Sergio, Pengfei, Jialu. I am sorry if I miss anyone.

Lastly, I want to show a deep appreciation to my family. My mum and dad support my research and always encourage me to be the best of myself. I only want to say: if possible, I still want to be your child in my next life.

Chapter One Introduction

1.1 Background

1.1.1 Molecular Nonlinear Optics (NLO)

Over the last decade, research into the use of photons as message carriers has been of increasing interest to the scientific community. The application of laser (light amplification by stimulated emission of radiation) technology, such as laser disc and scanners, has been widely studied and used in a range of products since the 1960s due to the research and exploitation of photoelectric materials that rely on the NLO (Nonlinear optical) effect.

In the field of NLO research, it is understood that the interaction between light and a substance generates several effects that include absorption and scattering. Under normal conditions, the optical effect is not related with the light intensity unlike the energy of the photons. When high intensity electromagnetic fields, including lasers, interact with matter, NLO effects are generated, which have a nonlinear relationship to light intensity. The substance exhibiting the above properties is known as NLO materials, which are widely used in optical communications, harmonic generators and electro-optic switches, along with new applications in biological imaging.[1] Chemists have the ability to design, synthesise and analyse different complexes to meet the demands of various NLO materials.

Practical NLO materials that exist as a single crystal are classed as inorganic. For example, β-barium borate (BBO: β-BaB_2O_4) created by the Fujian Institute of Research on the Structure of Matter, Chinese Academy of Sciences. Notably, it is not easily damaged while the transmittance region is approximately 200 to 2600 nm, which can be applied in frequency mixing and the frequency doubling of ultraviolet (UV) light.[2]

Furthermore, although the NLO coefficient of monopotassium phosphate (KDP: KH_2PO_4) is small, it has nevertheless been convenient to grow large KDP crystals that have been used for frequency doubling of powerful lasers. Meanwhile, potassium titanyl phosphate (KTP: $KTiOPO_4$) crystals have also been used for industrial applications. However, the NLO coefficient was found to be small and was very susceptible to optical damage. Investigations into molecular compounds is therefore now attracting attention, which include organometallic compounds; historically, these have been extensively used in harmonic generators to enhance the NLO effect[3] that arises from the great potential in molecular electronics and photonics.[4] In the past ten years, switchable quadratic NLO properties have also been studied using photo-excitation and redox reactions in organic and metalorganic molecular materials.[5]

Molecular NLO effects arise due to the hyperpolarisability response. At the micro scale, they are derived from the first hyperpolarisability (second-order) β and non-resonant response β_0 in addition to the second hyperpolarisability (third-order) γ. With respect to the non-resonant response β_0, it is connected to second-order NLO applications that usually avoid actual light absorption. From a macro perspective, the second-order β and third-order γ represent bulk susceptibilities $\chi^{(2)}$ and $\chi^{(3)}$ in the material respectively.

Second harmonic generation (SHG) is a good example of a macroscopic quadratic NLO process. SHG is also widely referred to as frequency doubling, and is an example of an NLO process. After the photon involved in the process breaks through the NLO material, it produces a frequency and energy two times greater than before, while the wavelength is halved. The non-zero value of $\chi^{(2)}$ usually requires a non-centrosymmetric structure and a polar order of molecules that are suitable for larger NLO effects. The design of the molecules, which includes these features, is consequently a huge challenge for the rearrangement and recombination of the polar sequence of elements. However, it is fortunate that the organic compounds are more suitable in comparison to inorganic counterparts because of the more convenient shape-changing nature of their structures; this notable characteristic applies in the case

of organometallic compounds.

In 1987, the Marder group were the first to discover a ferrocenyl derivative (cis)-[1-ferrocenyl-2-(4-nitrophenyl)ethylene] with a significant SHG coefficient.[6] Soon after, various experiments and theoretical studies then began to identify the second-order NLO properties of the organometallic compounds;[7-11] these included the new NLO materials that are now widely used today, which have also been investigated in this research. In comparison with inorganic complexes and purely organic compounds, organometallic compounds are more diverse in their electronic properties. There are currently numerous methods to change the second-order NLO properties. This approach of changing NLO properties can usually be achieved by changing the central metal species, the oxidation state of the metal and the surrounding coordination environment of the metal. The property of the ligand or the structure of the coordination complexes can also change second-order NLO properties.

1.1.2 Structural features

As previously discussed, the most suitable NLO material should possess high values of β and $\chi^{(2)}$. Based on numerous studies, the compound structures that exhibit these characteristics should be non-centrosymmetric. So at first, the molecular design was manipulated to synthesise a suspected non-centrosymmetric molecule, which resulted in a large β. Meanwhile, the crystal engineering method was attempted to gather these particles into a large macroscopic crystal. Synthetic chemists began experimenting with different reactions and obtained a new complex. The theoretical scientists employed various methods, such as the finite field or sum-over-state (SOS), to help describe the conditions that the molecule may need to satisfy. A significant body of research and experience has shown that the non-centrosymmetric molecule that has received an intra-molecular charge transition may lead to the presentation of an excellent NLO property. For example, molecules that possess a π bond typically also have a large β. If the electron-donating group and electron-withdrawing group are inserted into the right

place in the molecule, it would result in an asymmetric molecule distribution, which may further enhance the β and NLO properties. Based on the requirement of the second-order structure, the famous Donor-π-Acceptor (D-π-A) system was discovered. Here, D is an electron donor, π represents the π bond, and A represents for the electron acceptor. This system possesses a low energy metal-to-ligand charge transfer (MLCT) band. Typically, a charge transfer band in inorganic chemistry is related to the metal and divided into two groups: MLCT band and the ligand-to-metal charge transfer (LMCT) band. In the former, the electrons move from a molecular orbital of a metal to a ligand connected to a functional group. This band effect leads to an enormous β_0 and therefore represents an excellent NLO property. Furthermore, according to extensive experiments and theoretical studies, the second-order coefficients β and $\chi^{(2)}$, are proportional to the intensity of donor/acceptor and the conjugation length of the π system. However, research has also shown that this conjugation length has a limit; if too long, it will not improve the NLO property.[12-18]

It was acknowledged that the D-π-A system may possibly lead to a large β. Another issue in designing a suitable NLO property organometallic molecule was found to be the symmetry of organic molecule. Statistical data suggests that 75 per cent (%) of organic materials will be present as centro-symmetric crystals. This symmetry was unable to exhibit the macroscopic second-order NLO whilst simultaneously increasing the difficulty to grow the organic single crystal.[19] In fact, this long-term practice has led to the creation of some methods to make the organic molecules realise this non-centrosymmetric property in the material. The most popular of these is the anion-cation dual structure. In these materials, the cation is the main source of the NLO, while the anion adjusts the array of the cation chromophores by using the Coulomb force. Notably, a well-designed anion not only induces the non-centrosymmetric arrangement of cations but also optimises it to achieve the second largest macroscopic NLO property. This method produced the first commercial NLO material containing the anion-cation dual structure: the salt (E)-4’-(dimethylamino)-N-methyl-4-stilbazolium tosylate (DAST) (see Fig 1).[20-23] However, even though DAST possessed enhanced

NLO properties, it nevertheless constituted just 10 per cent of the result for the theoretical calculation. Moreover, the growth cycle of this crystal was quite long, which presented a challenge in its application.

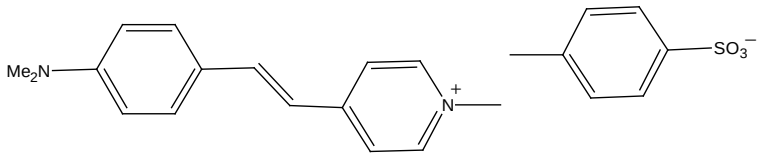

Fig 1. Structure of DAST

Recently, this area of research area has been divided into three groups, each taking one of the following approaches: (1) maintaining the cation in DAST and applying different anions.[24-26] New crystals were discovered and the NLO properties were compared to those of DAST, which were highly improved upon; (2) maintaining the anion in DAST and applying different cations.[27-29] However, the NLO properties of these materials did not exceed those of DAST. Meanwhile, the most common phenomenon was the more straightforward obtaining of the centro-symmetric structure after altering the cations; (3) changing both the cation and anion; Our group carried out this research and reported several new materials (such as DAPSH,[30] DAPSH: *trans*-4′-(dimethylamino)-*N*-phenyl-4-stilbazolium hexafluorophosphate), which possessed superior NLO properties in addition to excellent crystal growth abilities. Theoretical calculations and test results revealed that the NLO properties of these materials were larger in comparison to DAST;[30] however, the macroscopic NLO crystal was similar to that of DAST. This result indicated that the crystal packing was not perfect and still required improvement.

Multidimensional species, such as two-dimensions (2D) dipoles[31] and octupoles,[32] have a significant advantage in comparison to 1D (one dimension) dipoles. The most famous complexes are octupolar D_3 tris-chelates, which are based on $[M^{II}(bpy)_3]^{2+}$ (M = Fe, Ru, Zn, etc.; bpy= 2,2'-bipyridyl)[33] and 2D dipoles, which are mainly found with Schiff base ligands.[34]

Our group also investigated C_{2v} complexes, which included cis-$\{Ru^{II}(NH_3)_4\}^{2+}$ (an electron donor bonded to two pyridinium acceptors[35]) and two Ru^{II} centres coupled with a pyrazinyl core (see Fig 2).[36] These C_{2v} compounds usually have an intense and low energy MLCT transition and generate a huge β_0, which presents good NLO character in the molecule.[35,36]

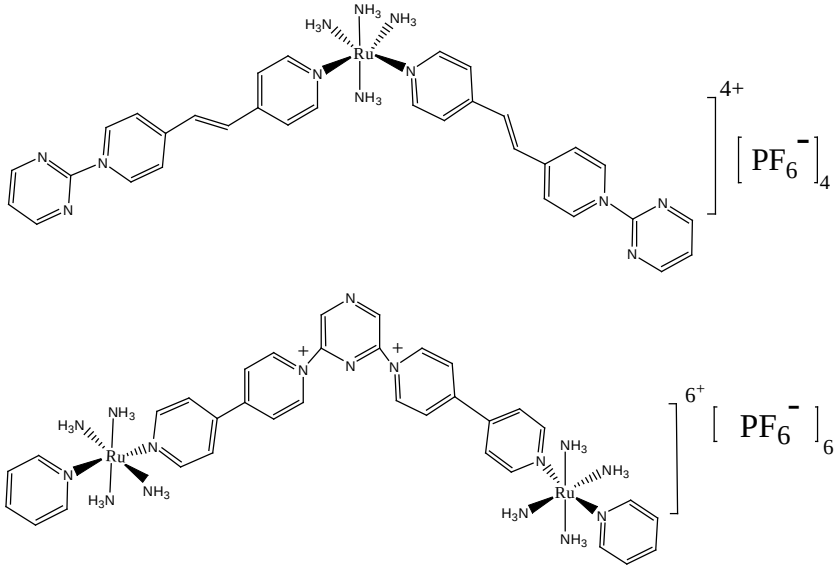

Fig 2. Examples of structure of C_{2v} complexes

1.1.3 Switching Nonlinear Optical Effects

In recent years, NLO switching has been widely studied. The protonation/deprotonation, oxidation/reduction, and photocyclisation processes gave the possibility of altering the NLO in addition to discovering the NLO switching. Both the protonation/deprotonation[37-39] and the oxidation/reduction[40] processes modify the properties of the donor or acceptor; the photocyclisation[41-43] process alters the extent of conjugation or the emission/absorption properties of the system.

The switching can be achieved by changing the NLO response of the molecule. In fact, amending the molecular structure of NLO materials for switching is challenging. The previous methods mainly involved isomerised or tautomerised molecules.[44] However,

the hyper-Rayleigh scattering (HRS) method was then invented,[45] which played a significant role in first detecting of hyperpolarisability. When a high strength laser started across the molecule, the second harmonic photons based on the incident light frequency were detected; this phenomenon called HRS,[45] and is a noncoherent second-order nonlinear scattering process, in which the frequency of scattered light was double that of the incident light. After the application of HRS, the reversible redox change in the D-π-A system of organometallic compounds and a β shift in the NLO response could be detected.[46] For performing protonation/deprotonation, the HRS technique was first used by the Hurst group[38] to describe the NLO switching of trans-bis(bidentate)phosphine ruthenium σ-arylvinylidene and σ-arylalkynyl complexes. The results revealed that this process caused a transformation between the alkynyl and vinylidene forms of the compound, in addition to causing the distinct change in β from 441×10^{-30} esu to 77×10^{-30} esu (see Fig 3).

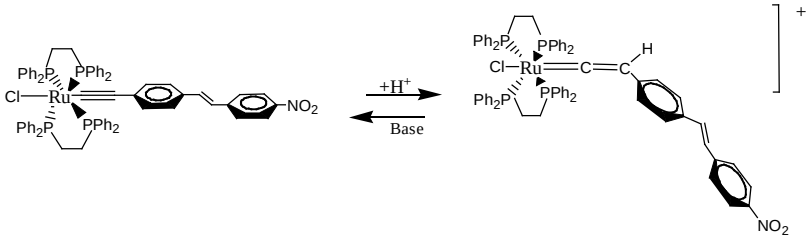

Fig 3. Transformation between alkynyl and vinylidene ligands

Meanwhile, during the investigation of photocyclisation, the Ordronneau group[42] conducted research into photochromic complexes (see Fig 4). The HRS revealed the point at which the ring of the listed compound opened i.e. when the β is 325×10^{-30} esu. However, the ring of this complex closed in response to UV light, which showed a very large β (1113×10^{-30} esu). Clearly, the open-ring form was the NLO "off" state, while the closed-ring form was the NLO "on" state. It was concluded that the closed-ring form could enhance the π electron de-localisability also in addition to the intensity of conjugation, which initiates the growth of β.

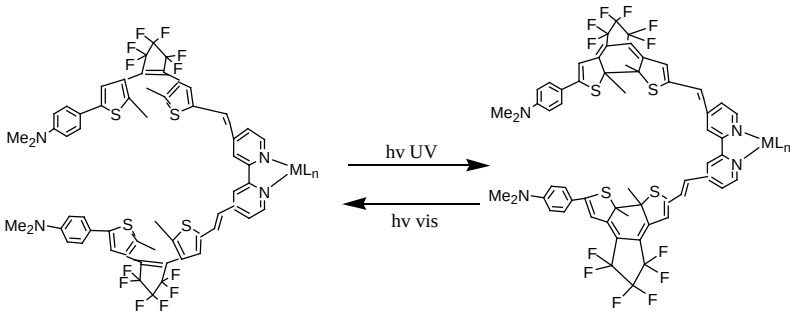

Fig 4. Photocyclization reaction

The redox switching of the linear optical absorption about the self-assembled monolayers of the Ru^{II} amines on platinum[47] and a $[Ru^{II}(bpy)_3]^{2+}$ derivative on ITO[48] (Indium tin oxide) have also been studied. The latest report involves SHG switching by absorbing carbon dioxide (CO_2) into a metal-organic framework[49] and β switching in a photochromic dye on metal binding,[50] which emphases the significance of the switching effects.

It was concluded that after the altering properties of the molecule had been discovered e.g. in the redox behaviors of metals, the switching NLO effects occurred.

1.2 β switching of C_{3v} chromophores in LB film

C_{2v} complexes have been widely studied, as in the case of the two pyridium acceptors previously described. Tracing the molecular NLO research reveals that systems possessing C_{3v} symmetry have not been explored to the same extent. The investigation into C_{3v} complexes thus became necessary, which began by studying subphthalocyanine (see Fig 5),[51] where it was reported that it was found to be electronically rich with an octupolar D_{3h} chromophore.

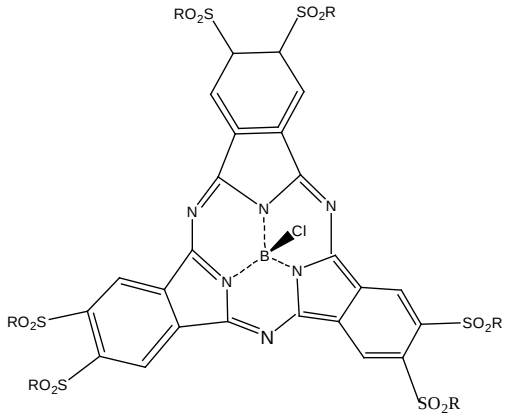

Fig 5. Structure of subphthalocyanine

Investigations have also been carried out into triarylphosphonium salt and triaryphosphine oxides with P^{+}-Me/P=O groups (see Fig 6).[52] Unfortunately, the results of the β_0 values were not improved by the aryl units and subsequently did not exhibit suitable NLO characteristics.

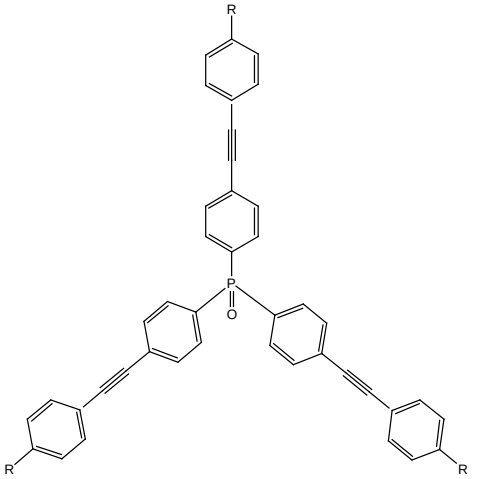

Fig 6. Structure of triaryphosphine oxides with P=O groups

In fact, only one study has addressed the facial geometry of an octahedral metal centre (Mn), which possess a C_{3v} symmetry (see Fig 7) and possibly includes a strong intraligand electronic coupling.[53]

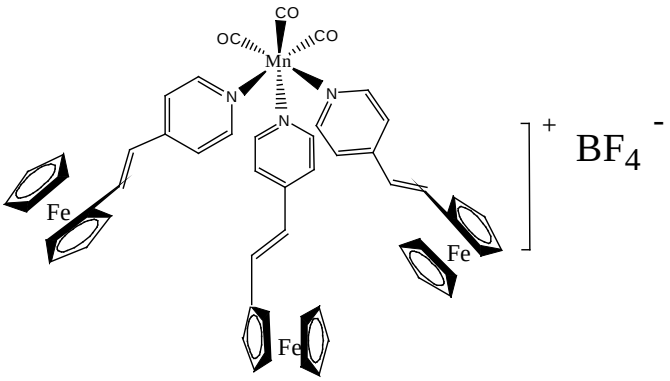

Fig 7. Structure of a manganese ion with localised C_{3v} symmetry

Our group attempted to synthesise non-organometallic complexes (containing 1,4,7-trithiacyclononane or tris(1-pyrazolyl)methane). However, synthetic problems prohibited us from successfully fashioning tripodal compounds that exhibited the required NLO activity.[54]

Investigations into the β switching theory were also initially carried out on the Ru^{II} ammine complexes by co-workers. It was discovered that it was possible to display a large β value and associate it with intense, low-energy MLCT excitation[55] through HRS.[56] Further detailed research revealed an association with the molecular quadratic and cubic NLO phenomena.[57]

Meanwhile, further research revealed that β could be reversibly modulated by the oxidation of the classic $[Ru^{II}(NH_3)_5L]^{3+}$ to $[Ru^{III}(NH_3)_5L]^{4+}$ (R= Alkyl chain) in addition to the reduction of $[Ru^{III}(NH_3)_5L]^{4+}$ to $[Ru^{II}(NH_3)_5L]^{3+}$ (see Fig 8).[58]

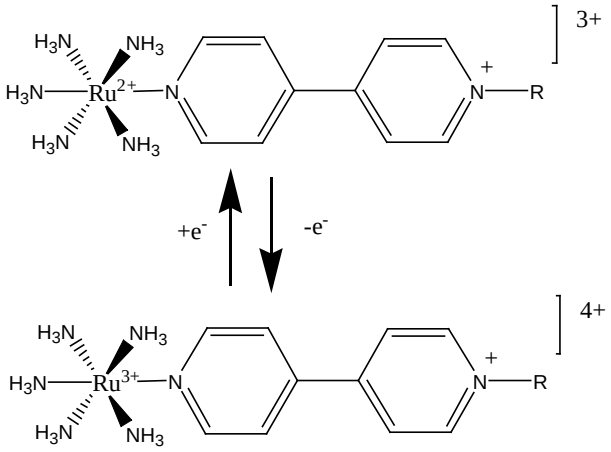

Fig 8. Redox behaviors of $[Ru^{X}(NH_3)_5L]^{Y}$ {X= 2, 3; Y=3, 4; R= Alkyl chain}.

It demonstrated that the β value could decrease from Ru^{II} to Ru^{III} and increase from Ru^{III} to Ru^{II}. The Ru^{III} mode revealed no low-energy charge-transfer absorptions due to the two opposing electron acceptors that attached to a pyridyl ring.[59] From Ru^{II} to Ru^{III}, the D-π-A system transferred to an Acceptor-π-Acceptor system. At this point, the β value could be controlled via redox, which made NLO switching feasible.

After the switchable NLO phenomenon was discovered, the research extended from materials towards applications that were related to Langmuir-Blodgett (LB) films that were used to produce polar arrangements of amphiphilic molecules.[60] This material contained non-centrosymmetric arrangements of active chromophores, which made it a polar material that must be electrochemically addressable and feasible to function as a thin film.

A LB film is made by transferring the monolayer of an organic material from a liquid to a solid substrate. This creates a significant advantage in terms of making a second-order NLO material, in that (1) the molecule can assemble freely; (2) the thickness of the film can be controlled at molecular level, either in a single layer or multiple layers; (3) the molecules in this film are arranged uniformly and in order; it is therefore not centro-symmetric. This unique character is well-suited to the demand of second-order NLO materials, namely that the molecule is required to be non-centrosymmetric.

Earlier research using Ru^{II} compounds (see Fig 9) involved their applications in SHG as part of LB films.[61]

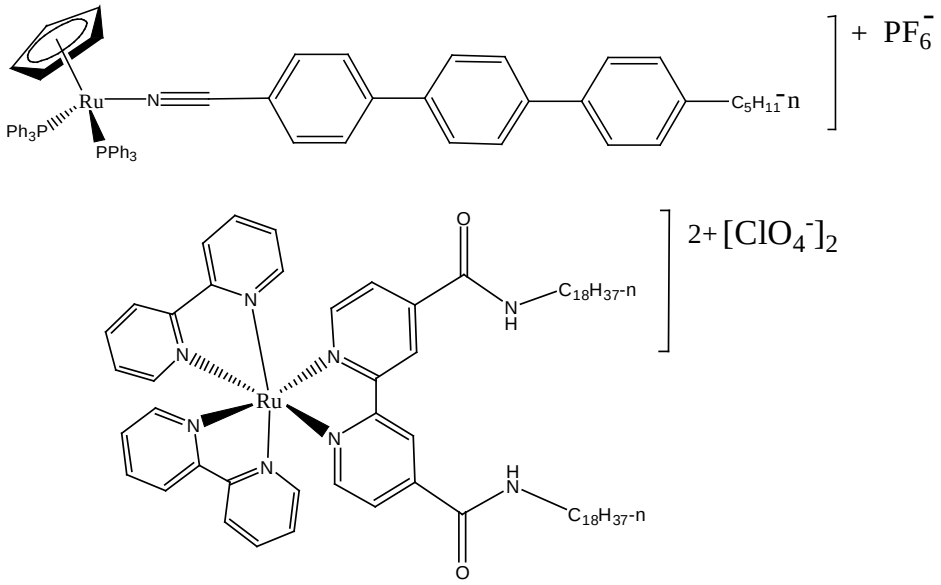

Fig 9. Structure of some Ru^{II} compounds used in LB films

Subsequently, another compound was found that satisfied the requirements identified by co-workers (see Fig 10).

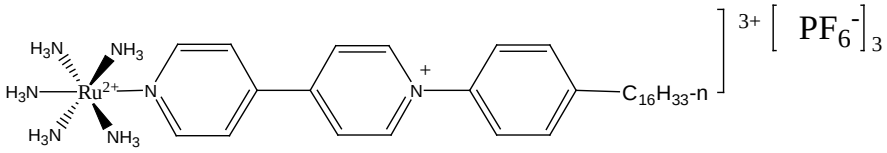

Fig 10. Structure of switching Ru^{II} complex in LB film

This compound was invented on a substrate of indium tin oxide (ITO)-coated glass by using the LB deposition technique. Its oxidation exhibited a sharp decline (by nearly 50 per cent) in SHG intensity in addition to a reduction that restored the SHG signal. However, the cycle was performed only twice before stopping, with the disappearance of the SHG signal.[62] Three aspects of this problem thus need to be addressed. The first involves the re-absorption of SHG by the Ru^{II} form. The second relates to the

incomplete oxidation brought about by the need for charge compensation resulting from anions moving from the electrolyte into the film and becoming isolated from the alkyl chains. Finally, the third aspect deals with the transformation of the film structure (or photodegradation).

1.3 Project objectives

This research aims to construct new "piano-stool" Ru^{II} complexes with three pyridinium-substituted ligands. This includes displaying the influence of NLO and rendering the complex salts amphiphilic nature by the long-chain alkyl substituents, which lead to high bulk NLO activities of switchable LB film. The main objectives are (1) the synthesis of a series of new C_{3v} chromophores and their characterisation by experimental and theoretical methods; (2) preparation of high quality LB films that exhibit large redox/photo-switching contrasts; (3) the refinement and optimisation of the electronic/optical properties and other application-relevant aspects (e.g. stability).

Chapter Two Piano-Stool Ruthenium (II) Complexes with Benzene Ring or Cymene Ring

2.1 Introduction

The final target of this project is to make LB films. However, based on our group previous studies, the challenges of preparing LB films of $[Ru(NH_3)_5]$ complexes are substantial. In fact, there were only one of nine salts that provided sufficiently high-quality multilayers.[58] Hence, identifying other types of compound was necessary. Based on the previous work in relation to the pseudolinear chromophore (Fig 11)[64] and a general survey of recent arene ring ruthenium complexes,[65,66] the results revealed that the ruthenium benzene and cymene [P-cymene (1-isopropyl-4-methylbenzene)] complexes were well studied. However, the research predominantly focused on 2,2'-bipyridyl compounds. The electronic spectroscopy and electrochemical properties of these were rarely investigated. Furthermore, the greatest interest in these complexes was concentrated on the theme as cancer-related drug. Therefore, advances in discovering electronic and redox properties for the designed compounds enabled the possibility of a greater array of meaningful end-user applications. Finally, the target tri-pyridyl complexes with a capping arene ring (benzene η^6-C_6H_6 or p-cymene η^6-$C_{10}H_{14}$) were intended to suit this aim.

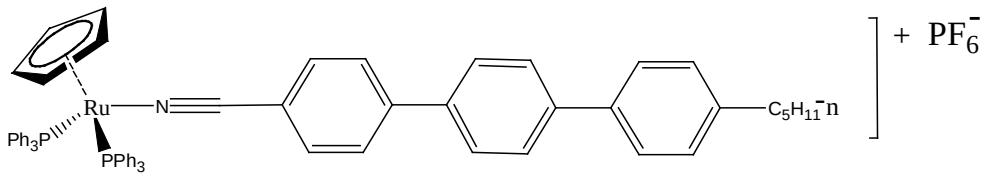

Fig 11 Ru^{II} complexes in LB film

The desired structure of the target compounds is illustrated in Figure 12. The ruthenium

plays a pseudo-octahedral coordination role in the centre so that the benzene ring and three identical pyridine/pyridyl ligands are able to occupy these coordination sites. In this kind of arene ruthenium piano-stool mononuclear complex $[(\eta^6$- arene$)Ru(L)_3]^{2+}$ (arene = benzene, η^6-C_6H_6, or p-cymene, η^6-$C_{10}H_{14}$; L= pyridine or pyridyl ligands), which are also known as half-sandwich ruthenium complexes, where the presence of the arene ring generates significant benefits in this system. For instance, the arene ring is relatively inert i.e. substitution reactions usually only occur at the three legs. The arene is a so-called spectator ligand. In summary, the arene ligands with π-acceptor pyridyl ligands may stabilise low oxidation states of ruthenium. By replacing the arene ring, it is possible to adjust the stability and redox properties of the complexes as well.

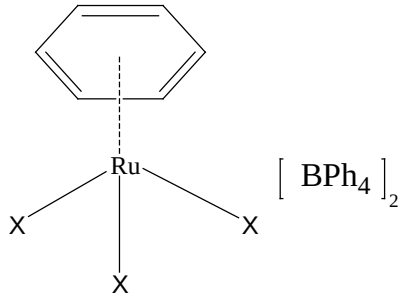

Fig 12. Designed structure (arene = benzene η^6-C_6H_6; X= pyridine or pyridyl ligands).

2.2 Experimental

2.2.1 Materials and Procedures

The compounds $[Ru(Bz)(N_2H_4)_3][BPh_4]_2$ (Bz: benzene) and $[Ru(Cym)(N_2H_4)_3][BPh_4]_2$ (Cym: cymene) were prepared according to published procedures.[63] All reactions were carried out under a nitrogen atmosphere and all solvents were degassed using nitrogen. Products were dried at room temperature overnight in a vacuum desiccator (SiO_2). All other reagents were obtained commercially and used as supplied.

2.2.2 General Physical Measurements

Mass spectra were recorded using a Thermo-Quest Finnigan Trace GC/MS or Thermo Electron Finnigan LTQ FT mass spectrometers. MALDI mass spectra were recorded using a micromass/Waters TOF spec 2E instrument. ^1H NMR (Nuclear magnetic resonance) spectra were recorded on Bruker Ultrashield 400 MHz and 500 MHz spectrometers, while all chemical shifts were quoted with respect to TMS. The microanalysis was conducted in collaboration with the School of Chemistry at the University of Manchester (UK). UV-visible spectra were obtained by using a Shimadzu UV-2401 PC. Cyclic voltammetric measurements were carried out by using an Ivium CompactStat instrument. A single-compartment cell was used with a silver/silver chloride reference electrode, a glassy carbon working electrode and a Platinum-wire auxiliary electrode. Dry DCM and acetonitrile were used and $[N(C_4H_9\text{-}n)_4]PF_6$ was the supporting electrolyte. Solutions contained ca. 10^{-3} M analyte (0.1 M electrolyte) deaerated by purging with Nitrogen. All $E_{1/2}$ values were calculated from $(E_{pa} + E_{pc})/2$ at a specified scan rate.

2.2.3 Syntheses

$[Ru(Bz)(N_2H_4)_3][BPh_4]_2$, [1]

To the purchased $[Ru(Bz)Cl_2]_2$ (0.2g, 0.40 mmol) in methanol (10 mL) was added hydrazine hydrate (0.5 mL) and the mixture stirred for half an hour at room temperature. The resulting red solution was filtered and $NaBPh_4$ (0.8g, 2.34 mmol) was added to precipitate a pale-yellow solid, which was isolated by filtration and washed with water (20 mL) and recrystallised from acetonitrile/Diethyl ether to yield yellow crystals: 0.5 g, 63%; δ_H (CD_3CN) 7.30 (16 H, d, J = 1.4, BPh_4), 7.02 (16 H, t, J = 7.4, BPh_4), 6.87 (8 H, t, J = 7.2, BPh_4), 6.08 (6 H, s, $3NH_2$), 5.81 (6 H, s, C_6H_6), 3.66 (6 H, s, $3NH_2$). ES-MS, m/z (-ES): 319.2 ($[BPh_4]^-$). m/z (+ES): 275 ($[M]^+$). Anal. Calcd (%) for $C_{54}H_{58}N_6B_2Ru$: C, 70.98; H, 6.40; N, 9.20. Found: C, 71.23; H, 6.44; N, 9.10.

$[Ru(Bz)(py)_3][BPh_4]_2$, [2] (py: pyridine)

To $[Ru(Bz)(N_2H_4)_3](BPh_4)_2$ (0.2 g, 0.22 mmol) in acetone (10 mL) was added pyridine (0.5 mL) and the solution stirred for 3 h at room temperature. Reduction in volume of the solution in vacuo led to the deposition of yellow crystals of $[Ru(Bz)(py)_3](BPh_4)_2$: 0.13 g, 55%; δ_H (DMSO) 8.49 (6 H, d, J = 5.4, C_5H_5N-$H^{2,6}$), 8.17 (3 H, t, J = 7.5, C_5H_5N-H^4), 7.62 (6 H, t, J = 6.9, C_5H_5N-$H^{3,5}$), 7.21 (16 H, s, BPh_4), 6.96 (16 H, t, J = 7.3, BPh_4), 6.82 (8 H, t, J = 7.0, BPh_4), 6.29 (6 H, s, C_6H_6). ES-MS, m/z (-ES): 319.2 ($[BPh_4]^-$). m/z (+ES): 338.1 ($[M - C_6H_6]^+$), 258.0 ($[M - 2C_6H_6]^+$). Anal. Calcd (%) for $C_{69}H_{61}N_3B_2Ru \cdot 3/2H_2O$: C, 77.16; H, 6.00; N, 3.91. Found: C, 76.80; H, 6.01; N, 3.80.

$[Ru(Bz)(pic)_3][BPh_4]_2$, [3] (pic: 4-picolline)

$[Ru(Bz)(N_2H_4)_3](BPh_4)_2$ (0.50g, 0.55 mmol) and 4-picolline (0.15 mL) were stirred in acetone (5 mL) for 3 h at room temperature. The crude product precipitated by adding diethyl ether. The final product was purified by silica column with eluent DCM:acetone

(dry)= 95:5, yield: 0.25 g, 42%; δ_H (CD_3CN) 8.11 (6 H, d, *J* = 6.7, C_5H_4N) 7.34 (6 H, d, *J* = 6.0, C_5H_4N), 7.32 – 7.26 (16 H, m, BPh_4), 7.02 (16 H, t, *J* = 7.4, BPh_4), 6.86 (8 H, t, *J* = 7.2, BPh_4), 6.02 (6 H, s, C_6H_6), 2.48 (9 H, s, NC_5H_4-C*H*$_3$). ES-MS, m/z (-ES)= 319.2 ($[BPh_4]^-$). m/z(+ES)= 229.5 ($[M]^+$), 366.0 ($[M - C_6H_7N]^+$), 272.0 ($[M - 2C_6H_7N]^+$). Anal. Calcd (%) for $C_{72}H_{67}N_3B_2Ru$: C, 78.83; H, 6.15; N, 3.83. Found: C, 78.43; H, 6.29; N, 3.80.

$[Ru(Bz)(ein)_3][BPh_4]_2$, [4] (ein: Ethyl isonicotinate)

$[Ru(Bz)(N_2H_4)_3](BPh_4)_2$ (0.5g, 0.55 mmol) was stirred with ethyl isonicotinate (0.24 mL) in acetone (5 mL) for 3 h at room temperature. The crude product precipitated by adding diethyl ether. The final product was purified by silica column with DCM:acetone(dry)= 95:5 as eluent, yield: 0.3g, 44%; δ_H (CD_3CN) 8.49 – 8.46 (6 H, m, C_5H_4N), 7.96 – 7.92 (6 H, m, C_5H_4N), 7.30 (16 H, m, BPh_4), 7.02 (16 H, t, *J* = 7.4, BPh_4), 6.87 (8 H, t, *J* = 7.2, BPh_4), 6.14 (6 H, s, C_6H_6), 4.44 (6 H, q, *J* = 7.1, OCH_2), 1.40 (9 H, t, *J* = 7.1, OCH_2-C*H*$_3$). ν(C=O)1715st cm^{-1}. ES-MS, m/z (-ES)= 319.2 ($[BPh_4]^-$). m/z(+ES)= 316.4 ($[M]^+$), 482.1 ($[M - C_8H_9NO_2]^+$), 330.0 ($[M - 2 C_8H_9NO_2]^+$), 453.1 ($[M - Ru - C_6H_6]^+$). Anal. Calcd (%) for $C_{78}H_{73}N_3O_6B_2Ru{\cdot}2H_2O$: C, 71.67; H, 5.93; N, 3.31. Found: C, 71.92; H, 5.58; N, 3.21.

$[Ru(Bz)(ppy)_3][BPh_4]_2$, [5] (ppy: 4-Phenylpyridine)

$[Ru(Bz)(N_2H_4)_3](BPh_4)_2$ (0.20g, 0.22 mmol) and 4-phenylpyridine (0.10 g) were stirred in acetone (5 mL) for 6 h at room temperature. The final product was obtained directly by adding diethyl ether: 0.23g, 82%; δ_H (Acetone) 8.67 – 8.63 (6 H, m, $C_{11}H_9N$), 7.82 – 7.69 (12 H, m, $C_{11}H_9N$), 7.47 – 7.41 (9 H, m, $C_{11}H_9N$), 7.24 – 7.16 (16 H, m, BPh_4), 6.78 (16 H, t, *J* = 7.4, BPh_4), 6.64 (8 H, t, *J* = 7.2, BPh_4), 6.33 (6 H, s, C_6H_6). m/z (-ES)= 319.2 ($[BPh_4]^-$). ES-MS, m/z(+ES)= 322.4 ($[M]^+$), 490.1 ($[M - C_{11}H_9N]^+$), 334.1 ($[M - 2C_{11}H_9N]^+$). Anal. Calcd (%) for $C_{87}H_{73}N_3B_2Ru{\cdot}3H_2O$: C, 78.14; H, 5.95; N, 3.27. Found: C, 78.55; H, 5.79; N, 3.14. TGA (TGA: Thermogravimetric analysis)

indicates the loss of ca. 3 molecules of water from the compound upon heating.

[Ru(Cym)(N_2H_4)$_3$][BPh_4]$_2$, [6]

To the purchased [Ru(Cym)Cl_2]$_2$ (0.2g, 0.33 mmol) in tetrahydrofuran (10 mL) was added hydrazine hydrate (0.5 mL) and the mixture stirred for 0.5 h at room temperature. The resulting solution was added to $NaBPh_4$ (0.8g, 2.34 mmol) to give a yellow solution. Then it was dried by vacuo and washed with DCM (10 mL). The yellow solid was isolated by filtration and washed with water (20 mL): 0.78 g, 98 %; δ_H (CD_3CN) 7.33 – 7.26 (16 H, m, BPh_4), 7.03 (16 H, t, *J* = 7.4, BPh_4), 6.87 (8 H, t, *J* = 7.2 BPh_4), 5.91 (6 H, s, 3NH_2), 5.74 (2 H, d, *J* = 6.2, C_6H_4), 5.52 (2 H, d, *J* = 6.2, C_6H_4), 3.62 (6 H, s, 3NH_2), 2.86 (1H, septet, *J* = 6.8, C*H*(CH_3)$_2$), 2.20 (3 H, s, C_6H_4-C*H*$_3$), 1.27 (6 H, d, *J* = 6.9, CH(C*H*$_3$)$_2$). ES-MS, m/z (-ES): 319.2 ([BPh_4]$^-$). m/z (+ES): 299 ([M − N_2H_4]$^+$), 267 ([M − 2N_2H_4]$^+$), 235 ([M − 3N_2H_4]$^+$). Anal. Calcd (%) for $C_{58}H_{66}N_6B_2Ru\cdot N_2H_4$: C, 69.53; H, 7.04; N, 11.18. Found: C, 68.93; H, 7.35; N, 10.78.

[Ru(Cym)(py)$_3$][BPh_4]$_2$, [7]

[Ru(Cym)(N_2H_4)$_3$][BPh_4]$_2$ (0.5g, 0.51 mmol) in acetone (25 mL) was added to pyridine (0.2 mL) and the solution stirred for 3 h at room temperature. The yellow product [Ru(Cym)(py)$_3$](BPh_4)$_2$ was obtained by recrystallization from acetonitrile/diethyl ether: 0.35 g, 61%; δ_H (CD_3CN) 8.29 (6 H, d, *J* = 5.2, C_5H_5N-H^{2,6}), 8.10 (3 H, t, *J* = 7.7, C_5H_5N-H^4), 7.53 (6 H, dd, *J* = 7.5, 6.7, C_5H_5N-H^{3,5}), 7.33 – 7.26 (16 H, m, BPh_4), 7.02 (16 H, t, *J* = 7.4, BPh_4), 6.87 (8 H, t, *J* = 7.2, BPh_4), 6.04 (2 H, d, *J* = 6.4, C_6H_4), 5.87 (2 H, d, *J* = 6.4, C_6H_4), 3.45 (1 H, septet, *J* = 7.0, C*H*(CH_3)$_2$), 1.64 (3 H, s, C_6H_4-C*H*$_3$), 1.04 (6 H, d, *J* = 6.9, CH(C*H*$_3$)$_2$). ES-MS, m/z (-ES): 319.2 ([BPh_4]$^-$). m/z (+ES): 393 ([M − C_5H_5N]$^+$), 314.1 ([M − 2C_5H_5N]$^+$), 237.1 ([M − Ru − $C_{10}H_{14}$]$^+$). Anal. Calcd (%) for $C_{73}H_{69}N_3B_2Ru\cdot 5H_2O$ from microanalysis: C, 72.99; H, 6.62; N, 3.49. Found: C, 72.43; H, 5.92; N, 3.69.

[Ru(Cym)(pic)$_3$][BPh$_4$]$_2$, [8]

[Ru(Cym)(N$_2$H$_4$)$_3$][BPh$_4$]$_2$ (0.20g, 0.21 mmol) and 4-picolline (0.06 mL) were stirred in acetone (10 mL) for 3 h at room temperature. The crude product was precipitated by adding diethyl ether. The final product was purified by silica column with an eluent of DCM:acetonitrile (dry)= 95:5: 0.10 g, 44%; δ_H (DMSO) 8.24 (6 H, d, *J* = 6.4, C$_5$H$_4$N), 7.45 (6 H, d, *J* = 6.2, C$_5$H$_4$N), 7.17 (16 H, s, BPh$_4$), 6.92 (16 H, t, *J* = 7.4, BPh$_4$), 6.79 (8 H, t, *J* = 7.2, BPh$_4$), 6.29 (2 H, d, *J* = 6.3, C$_6$H$_4$), 6.05 (2 H, d, *J* = 6.3, C$_6$H$_4$), 2.45 (9 H, s, NC$_5$H$_4$-C*H*$_3$), 2.07 (1H, septet, J = 6.6, C*H*(CH$_3$)$_2$), 1.59 (3 H, s, C$_6$H$_4$-C*H*$_3$), 0.98 (6 H, d, *J* = 6.9, CH(C*H*$_3$)$_2$). ES-MS, m/z (-ES): 319.2 ([BPh$_4$]$^-$). m/z (+ES): 422.2 ([M − C$_6$H$_7$N]$^+$), 328.1 ([M − 2C$_6$H$_7$N]$^+$), 228.3 ([M − Ru − 2C$_6$H$_7$N]$^+$). Anal. Calcd (%) for C$_{76}$H$_{75}$N$_3$B$_2$Ru: C, 79.16; H, 6.55; N, 3.64. Found: C, 78.65; H, 6.01; N, 3.71.

[Ru(Cym)(ein)$_3$][BPh$_4$]$_2$, [9]

[Ru(Cym)(N$_2$H$_4$)$_3$][BPh$_4$]$_2$ (0.5g, 0.51 mmol) was stirred with ethyl isonicotinate (0.22 mL) in acetone (5 mL) for 3 h at room temperature. The crude product was precipitated by adding diethyl ether. The final product was purified by silica column with an eluent of DCM:acetone(dry)= 95:5: 0.30g, 44%; δ_H (DMSO) 8.66 (6H, d, *J* = 6.5, C$_5$H$_4$N), 7.92 (6H, d, *J* = 6.5, C$_5$H$_4$N), 7.17 (16H, s, BPh$_4$), 6.92 (16H, t, *J* = 7.3, BPh$_4$), 6.79 (8H, t, *J* = 7.1, BPh$_4$), 6.44 (2H, d, *J* = 6.3, C$_6$H$_4$), 6.22 (2H, d, *J* = 6.3, C$_6$H$_4$), 4.40 (6H, q, *J* = 7.0, OCH$_2$), 2.13 (1H, septet, J = 6.6, C*H*(CH$_3$)$_2$), 1.64 (3H, s, C$_6$H$_4$-C*H*$_3$), 1.33 (9H, t, *J* = 7.1, OCH$_2$-C*H*$_3$), 1.00 (6H, d, *J* = 6.8, CH(C*H*$_3$)$_2$). ν(C=O)1705st cm^{-1}. ES-MS, m/z (-ES)= 319.2 ([BPh$_4$]$^-$). (m/z(+ES)= 344.6 ([M]$^+$), 583.2 ([M − C$_8$H$_9$NO$_2$]$^+$), 386.1 ([M – 2 C$_8$H$_9$NO$_2$]$^+$), 555.2 ([M − C$_{10}$H$_{14}$]$^+$). Anal. Calcd (%) for C$_{82}$H$_{81}$N$_3$O$_6$B$_2$Ru·2H$_2$O: C, 72.24; H, 6.28; N, 3.08. Found: C, 72.44; H, 6.25; N, 3.16.

[Ru(Cym)(ppy)$_3$][BPh$_4$]$_2$, [10]

[Ru(Cym)(N$_2$H$_4$)$_3$][BPh$_4$]$_2$ (0.20g, 0.21 mmol) and 4-phenylpyridine (0.10 g) were stirred in acetone (5 mL) for 6 h at room temperature. The final product was obtained directly by adding diethyl ether: 0.20 g, 71%; δ_H (DMSO) 8.55 (6 H, d, *J* = 6.9, C$_{11}$H$_9$N), 8.03 – 7.94 (12 H, m, C$_{11}$H$_9$N), 7.60 (9 H, dd, *J* = 5.0, 1.8, C$_{11}$H$_9$N), 7.22 – 7.14 (16 H, m, BPh$_4$), 6.92 (16 H, t, *J* = 7.4, BPh$_4$), 6.79 (8 H, t, *J* = 7.2, BPh$_4$), 6.44 (2 H, d, *J* = 6.4, C$_6$H$_4$), 6.22 (2 H, d, *J* = 6.4, C$_6$H$_4$), 2.09 (1 H, septet, J = 6.5, C*H*(CH$_3$)$_2$), 1.71 (3 H, s, C$_6$H$_4$-C*H*$_3$), 1.04 (6 H, d, *J* = 6.9, CH(C*H*$_3$)$_2$). ES-MS, m/z (-ES)= 319.2 ([BPh$_4$]$^-$). m/z(+ES)= 350.4 ([M]$^+$), 546.2 ([M – C$_{11}$H$_9$N]$^+$), 465.1 ([M – Ru – C$_{10}$H$_{14}$]$^+$) 390.1 ([M – 2C$_{11}$H$_9$N] $^+$). Anal. Calcd (%) for C$_{91}$H$_{81}$N$_3$B$_2$Ru·2H$_2$O: C, 79.47; H, 6.23; N, 3.05. Found: C, 79.72; H, 6.21; N, 3.38.

2.2.4 X-Ray Crystallography

Crystals of [Ru(Bz)(N$_2$H$_4$)$_3$][BPh$_4$]$_2$ and [Ru(Cym)(N$_2$H$_4$)$_3$][BPh$_4$]$_2$ were obtained by slow diffusion of diethyl ether into a nitromethane solution. [Ru(Bz)(py)$_3$][BPh$_4$]$_2$ was obtained by slow diffusion of diethyl ether into DMF solution. Crystals of [Ru(py)$_3$(DMF)$_3$][BPh$_4$]$_2$ were obtained as a decomposition product during the crystallization of [Ru(Bz)(py)$_3$][BPh$_4$]$_2$. Dr J. Raftery solved all crystal structures at The University of Manchester except for [Ru(py)$_3$(DMF)$_3$][BPh$_4$]$_2$ and [Ru(Bz)(py)$_3$][BPh$_4$]$_2$, which were solved by Dr Sergio Sanchez.

2.3 Results and Discussion

2.3.1 Synthetic Characterization Studies

The new ruthenium (II) piano-stool complexes with three monodentate pyridine or pyridyl ligands, **1-10**, were synthesised and entirely characterised. These compounds were designed to investigate the basic coordination chemistry with simple ligands prior to moving on to functional derivatives, which included the electronic and redox properties.

Our group began the study of the simple ligands, which related to the basic coordination chemistry and $[Ru(Bz)Cl_2]_2$ (see Fig 13), which was vital to the synthesis of the "piano-stool" complexes so it was chosen as the starting material.

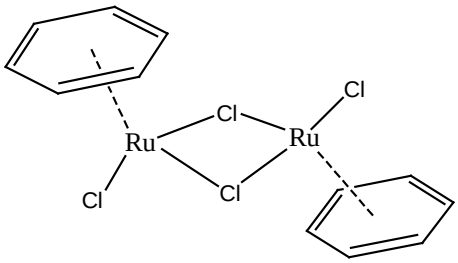

Fig 13. Structural formula of benzene ruthenium chloride dimer.

$[Ru(Bz)Cl_2]_2$ was first reported by Winkhaud and Singer in 1967[67] as a result of the reaction between $RuCl_3.xH_2O$ with 1,3-cyclohexadiene in ethanol to produce a brown solid $[Ru(Bz)Cl_2]_2$. In 1972, this method was improved upon by Zelonka and Baird who produced a superior yield; notably, they challenged the brown insoluble product that was created by Winkhaud and Singer as being unreactive.[68] This method became more mature after further discoveries by Bennett and Smith.[69,70] The fundamental difference was in the choice of the reaction solvent. In the method described by Bennett and Smith, both 1,3-cyclohexadiene and 1,4-cyclohexadiene (see Fig 14) were used to synthesise the dimer, which resulted in no difference.

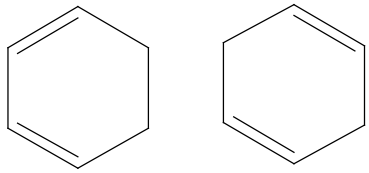

Fig 14. Structural formulae of 1,3-cyclohexadiene and 1,4-cyclohexadiene.

Bennett and Smith also conducted a study into the reaction temperature. They reported that nothing occurred when $RuCl_3$ and 1,4-cyclohexadiene reacted at room temperature. However, under the same conditions, over a couple of days, 1,3-cyclohexadiene and $RuCl_3$ led to precipitation of $[Ru(Bz)Cl_2]_2$. Bennett and Smith concluded that this was due to the isomerization of 1,4-cyclohexadiene to 1,3-cyclohexadiene before dehydrogenation took place. More Recently, repetition of this method (with slight modifications) by Myahkostupov[71] and Abbotto[72] produced a higher yield in comparison to earlier methods (see Fig 15). Notably, both approaches used 1,3-cyclohexadiene and 1,4-cyclohexadiene as the starting material. However, they applied different reaction temperatures: 85℃ and 45℃ respectively. The reaction time also differed slightly, at 4 hours and 3 hours respectively.

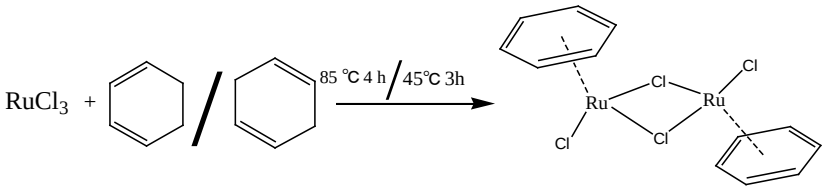

Fig 15. Reaction for synthesis of benzene ruthenium chloride dimer.

Another novel method developed to synthesise the dimer involved microwave heating, which produced some advantages. With progress in microwave chemistry, the dimer $[Ru(Bz)Cl_2]_2$ was first produced by Baghurst and Mingos,[73] using microwave heating as the synthetic method instead of conventional reflux. This reduced the reaction time to approximately 30 minutes. Sun and Machala[74] further improved the use of this approach for similar compounds, such as $[Ru(Cym)Cl_2]_2$. The most recent advance was made by

Justus[75] in 2013, who reported that microwave heating could be applied for the synthesis of many $[(\pi\text{-ligand})RuCl_2]_2$ complexes. In summary, this method has advantages over the traditional method, which include: less solvent, sometimes less ligand precursor as the reactant and, most importantly, a shorter reaction time. Conversely, the method is comparatively expensive due to the high cost of the machine and the raw materials.

In order to produce a more effective reaction and minimise the cost, 1,4-cyclohexadiene (10 mL) was chosen to react with $RuCl_3 \cdot xH_2O$ (2.00 g) in ethanol (100 mL) at 85℃ for 4.5 hours. Red solids (1.83 g) were obtained, which was a similar yield to that of Bennett.[69,70] However, the characterisation results showed that the compound was insufficiently pure. Therefore, it was not an appropriate starting material and would likely affect the subsequent purity of the target compounds. Commercial $[Ru(Bz)Cl_2]_2$ and $[Ru(Cym)Cl_2]_2$ were therefore finally selected as the starting materials to avoid the presence of impurities. These dimers were then used as precursors for generating $[Ru(Bz)(N_2H_4)_3][BPh_4]_2$ and $[Ru(Cym)(N_2H_4)_3][BPh_4]_2$, which were the first C_{3v} symmetry complexes.[63] The full synthetic steps are shown below (See Scheme 1).

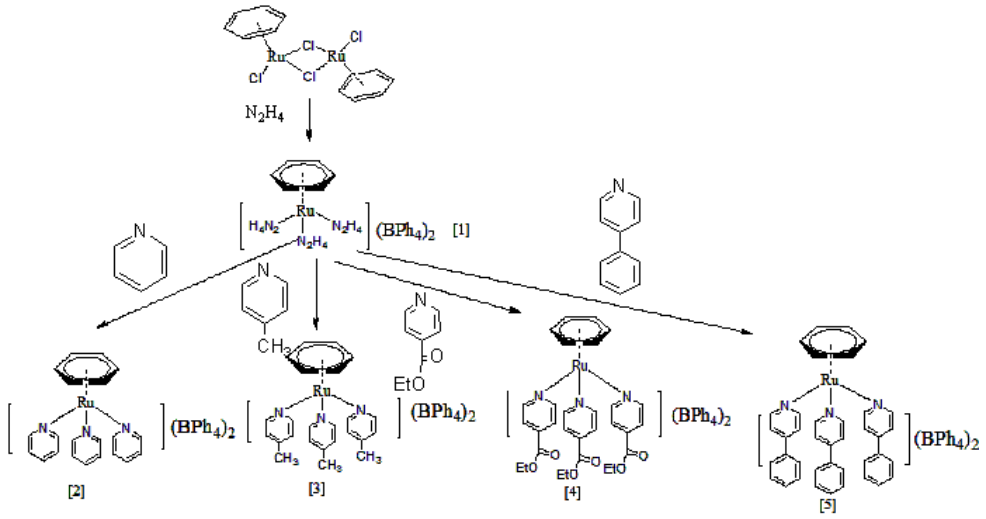

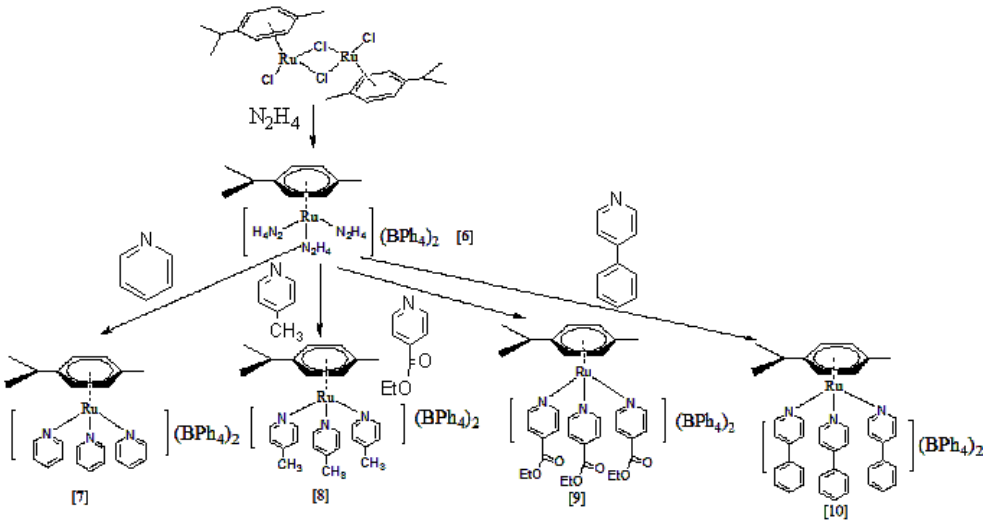

Scheme 1. Synthesis of compounds [1-10].

For complexes (**3-5)** there existed purification problems. Various eluents with either silica or alumina columns were therefore trialed. One low-efficiency eluent system was found to be acetone: water: saturated aqueous KNO_3= 16:4:1, although the difficulty of precipitating the products leads to inadequate quantities for subsequent characterisation. Ion exchange of BPh_4^- (BPh_4: Tetraphenylborate) to PF_6^- or BF_4^- was tried as well. However, it did not work due to lack of precipitation.

For compounds (**8-10)** there were also impurity issues. After different eluents with either silica or alumina column were unsuccessfully attempted, another direct synthesis method was developed. Several research groups have studied different direct methods that began from $[Ru(Cym)Cl_2]_2$ to generate $[Ru(Cym)Cl(L)_2]$ or $[Ru(Cym)Cl_2(L)]$ (L=pyridyl group).[76] Meanwhile, several chelate complexes from $[Ru(Cym)Cl_2]_2$ have also been fabricated.[77] The direct method of synthesising $[Ru(Cym)(L)_3]^{2+}$ was formed by using $[Ru(Cym)Cl_2]_2$ as the starting material, which was first introduced by Carmona.[78] $AgBF_4$ in addition to the ligand were then added to obtain the crude product. The final product was recrystallised from DCM/diethyl ether. The Vock group[79] followed this method to create another similar compound $[Ru(\eta^6\text{-benzene})(mimid)_3][BF_4]_2$ (mimid= N-methylimidazole). Other groups (such as

Wallace[80,81]) also carried out similar synthesis experiments by using $AgPF_6$ or $AgBF_4$. Based on the logic of this methodology, the direct method was a worthwhile trial, especially considering the faster reaction time. Therefore, the modified method was trialed by using $AgBF_4$. However, the results indicated that the methodology was not suitable for our target complex. The NMR spectrum results revealed that the data was in fact a mixture, so another purification method developed. Firstly, different recrystallisation solvent systems were trialed but unfortunately each failed. Secondly, both silica and alumina columns were attempted separately. Different coloured bands could be observed on the column, which indicated that at least two impurities were present in this product. The results of the separation by column continued to be unsuccessful, which could be attributed to the solubility and stability of this complex. In relation to the C_{3v} symmetry structure, the BF_4^- salts may not have been sufficiently stable, which made changing the anion essential. Next, PF_6^- and BPh_4^- were attempted – but unfortunately failure ensued. In general, the direct method using $AgPF_6$ or $AgBF_4$ to synthesise compounds (**5-10)** was not successful. Another novel method was subsequently attempted that incorporated the Sephadex column CMC-25 and SPC-25[82] with the eluent (NaCl: Acetone=1:1, 5:3) or (HCl=0.1M-0.9M); the target complex merely decomposed on the column. However, a straightforward and efficient eluent was found to be DCM: acetone(dry)=95:5. This practical method finally purified the complexes (**3-5**, **8-10)**.

The reaction of $[Ru(Bz)(N_2H_4)_3][BPh_4]_2$ or $[Ru(Cym)(N_2H_4)_3][BPh_4]_2$ with pyridine or pyridyl ligands in acetone at room temperature after purification by silica column chromatography resulted in the formation of new arene ruthenium piano-stool pyridine or pyridyl complexes. These complexes were all stable in air and were soluble in polar solvents such as acetone and dichloromethane. However, they were insoluble in diethyl ether and hexane. The diamagnetic nature of all of these complexes was consistent with the +2 oxidation state. For compounds (**1-10)**, NMR data showed that the complexes are highly pure. The electrospray mass spectrometry revealed the existence of all complexes and the elemental analyses were consistent with the composition proposed for all

complexes. Thermogravimetric analysis (TGA) of **5** indicated the loss of around three molecules of water upon heating, which is the 5.42% of its molecular weight. The infra-red spectra of **4** and **9** displayed a strong band around 1700 cm^{-1}, which corresponded to $\nu_{C=O}$ for these compounds.

2.3.2 ^{1}H NMR Spectroscopy Studies

The ^{1}H NMR spectra for all of the complexes are well defined when recorded in deuterated DMSO or CD_3CN or acetone solution to probe the solution structure (Table 1). A representative spectrum is shown in Figure 16.

Complexes	^{1}H NMR data (ppm, J in Hz)
1	7.30 (16 H, d, *J* = 1.4, BPh_4), 7.02 (16 H, t, *J* = 7.4, BPh_4), 6.87 (8 H, t, *J* = 7.2, BPh_4), 6.08 (6 H, s, $3NH_2$), 5.81 (6 H, s, C_6H_6)
2	7.21 (16 H, s, BPh_4), 6.96 (16 H, t, *J* = 7.3, BPh_4), 6.82 (8 H, t, *J* = 7.0, BPh_4), 6.29 (6 H, s, C_6H_6)
3	7.32 – 7.26 (16 H, m, BPh_4), 7.02 (16 H, t, *J* = 7.4, BPh_4), 6.86 (8 H, t, *J* = 7.2, BPh_4), 6.02 (6 H, s, C_6H_6)
4	7.30 (16 H, m, BPh_4), 7.02 (16 H, t, *J* = 7.4, BPh_4), 6.87 (8 H, t, *J* = 7.2, BPh_4), 6.14 (6 H, s, C_6H_6)
5	7.24 – 7.16 (16 H, m, BPh_4), 6.78 (16 H, t, *J* = 7.4, BPh_4), 6.64 (8 H, t, *J* = 7.2, BPh_4), 6.33 (6 H, s, C_6H_6)
6	7.33 – 7.26 (16 H, m, BPh_4), 7.03 (16 H, t, *J* = 7.4, BPh_4), 6.87 (8 H, t, *J* = 7.2 BPh_4), 5.74 (2 H, d, *J* = 6.2, C_6H_4), 5.52 (2 H, d, *J* = 6.2, C_6H_4), 2.86 (1 H, septet, *J* = 6.8, C*H*$(CH_3)_2$), 2.20 (3 H, s, C_6H_4-C*H*$_3$), 1.27 (6 H, d, *J* = 6.9, CH(C*H*$_3)_2$)
7	7.33 – 7.26 (16 H, m, BPh_4), 7.02 (16 H, t, *J* = 7.4, BPh_4), 6.87 (8 H, t, *J* = 7.2, BPh_4), 6.04 (2 H, d, *J* = 6.4, C_6H_4), 5.87 (2 H, d, *J* = 6.4, C_6H_4), 3.45 (1 H, septet, *J* = 7.0, C*H*$(CH_3)_2$), 1.64 (3 H, s, C_6H_4-C*H*$_3$), 1.04 (6 H, d, *J* = 6.9, CH(C*H*$_3)_2$)
8	7.17 (16 H, s, BPh_4), 6.92 (16 H, t, *J* = 7.4, BPh_4), 6.79 (8 H, t, *J* = 7.2, BPh_4), 6.29 (2 H, d, *J* = 6.3, C_6H_4), 6.05 (2 H, d, *J* = 6.3, C_6H_4), 2.07 (1H, septet, J = 6.6, C*H*$(CH_3)_2$), 1.59 (3 H, s, C_6H_4-C*H*$_3$), 0.98 (6 H, d, *J* = 6.9, CH(C*H*$_3)_2$)
9	7.17 (16H, s, BPh_4), 6.92 (16H, t, *J* = 7.3, BPh_4), 6.79 (8H, t, *J* = 7.1 , BPh_4), 6.44 (2H, d, *J* = 6.3, C_6H_4), 6.22 (2H, d, *J* = 6.3, C_6H_4), 2.13 (1H, septet, *J* = 6.6, C*H*$(CH_3)_2$), 1.64 (3H, s, C_6H_4-C*H*$_3$), 1.00 (6H, d, *J* = 6.8, CH(C*H*$_3)_2$)
10	7.22 – 7.14 (16 H, m, BPh_4), 6.92 (16 H, t, *J* = 7.4, BPh_4), 6.79 (8 H, t, *J* = 7.2, BPh_4), 6.44 (2 H, d, *J* = 6.4, C_6H_4), 6.22 (2 H, d, *J* = 6.4, C_6H_4), 2.09 (1 H, septet, *J* = 6.5, CH$(CH_3)_2$), 1.71 (3 H, s, C_6H_4-C*H*$_3$), 1.04 (6 H, d, *J* = 6.9, CH(C*H*$_3)_2$)

Table 1. Selected ^{1}H NMR data of complexes [1-10].

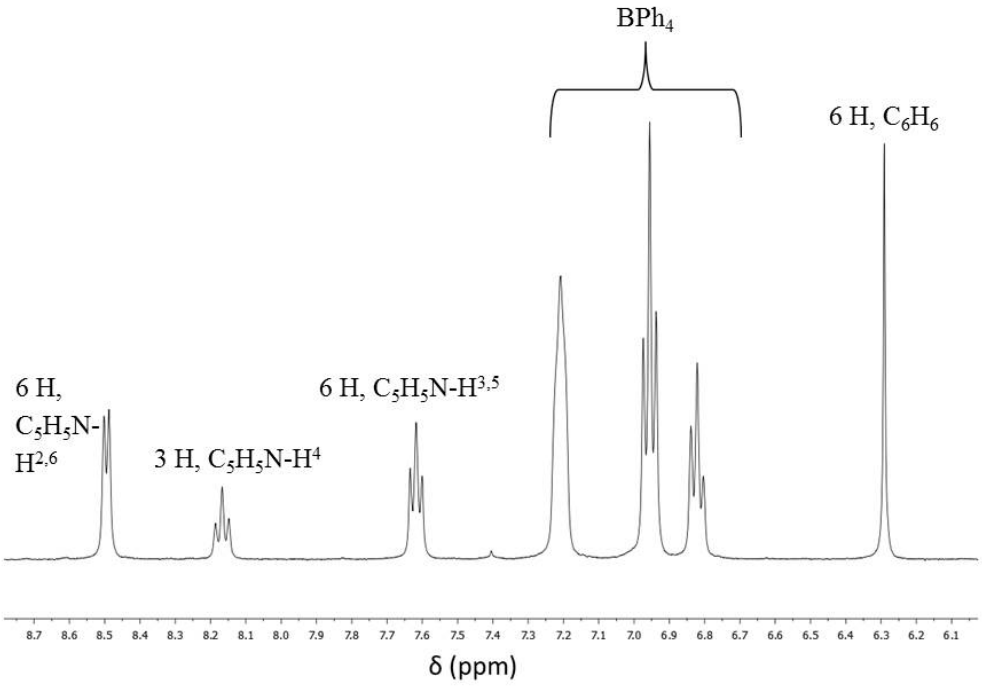

Fig 16. ^{1}H NMR spectrum (deuterated DMSO, 400MHz, room temperature) of 2 $[Ru(Bz)(py)_3][BPh_4]_2$.

All of the complexes show three peaks between δ 8 ppm and δ 6 ppm for the presence of BPh_4^-. The benzene ring protons appear as singlet around δ 6 ppm, while the p-cymene ring protons are observed in the range of δ 5-6 ppm as two doublets (2H). The methyl protons of p-cymene appear as a singlet and isopropyl protons of p-cymene appear in the range about δ 1 ppm. The isopropyl CH protons appear as a septet in the range of δ 2-3 ppm. The protons of pyridine or pyridyl ligands exhibit the peaks around δ 8-7 ppm. The NMR data reveal an upfield chemical shift of the ring hydrogen, which belong to the benzene or p-cymene moiety by comparison with the free aromatic ring (7.27 ppm);[83] this is ascribed to the π-backbonding of the ligand to ruthenium.[83] The rationale behind this theory is that the electron density moves from ruthenium to the arene ligands, which causes the strengthening shielding of ring hydrogens.

2.3.3 Electronic Spectroscopy Studies

The electronic absorption spectra of complexes (**1-10**) recorded in acetonitrile or DCM solution at room temperature are listed in Table 2. The spectra of complexes (**1,2,6,7,8**) and complexes (**3,4,5,9,10**) are shown in Figure 17 and 18, respectively.

Complexe	λ_{max}/ nm ($\varepsilon_{max}/10^3$ M^{-1} cm^{-1})	E_{max}/ eV	Assignment
1	267 (10)	4.64	MLCT ($\pi \rightarrow \pi^*$)
2	267 (21)	4.64	MLCT ($\pi \rightarrow \pi^*$)
3	228 (48)	5.43	$\pi \rightarrow \pi^*$
	267 (18)	4.64	MLCT ($\pi \rightarrow \pi^*$)
4	229 (54)	5.41	$\pi \rightarrow \pi^*$
	275 (17)	4.50	MLCT ($\pi \rightarrow \pi^*$)
5	228 (65)	5.43	$\pi \rightarrow \pi^*$
	295 (51)	4.20	MLCT ($\pi \rightarrow \pi^*$)
6	267 (9)	4.64	MLCT ($\pi \rightarrow \pi^*$)
7	266 (20)	4.66	MLCT ($\pi \rightarrow \pi^*$)
8	267 (15)	4.64	MLCT ($\pi \rightarrow \pi^*$)
9	228 (54)	5.43	$\pi \rightarrow \pi^*$
	275 (17)	4.50	MLCT ($\pi \rightarrow \pi^*$)
10	229 (63)	5.41	$\pi \rightarrow \pi^*$
	295 (52)	4.20	MLCT ($\pi \rightarrow \pi^*$)

Table 2. UV-Visible data for complexes [1-10] in acetonitrile[a] or DCM[b].

[a] Solutions ca $2.5x10^{-5}$ M. Complexes (**1, 2, 6, 7, 8**) measured in acetonitrile. [b] Solutions ca $2.5x10^{-5}$ M. Complexes (**3, 4, 5, 9, 10**) measured in DCM.

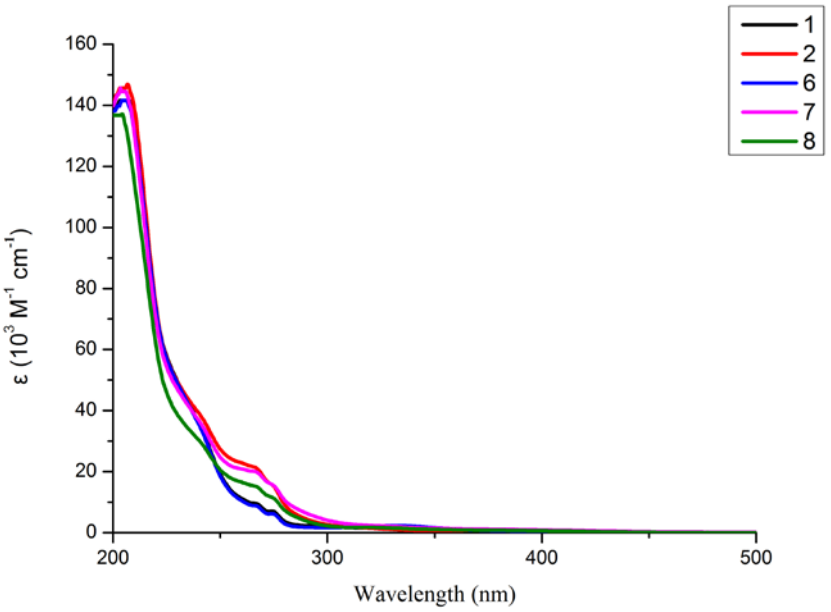

Fig 17. Electronic absorption spectra of complexes 1, 2, 6, 7, 8.

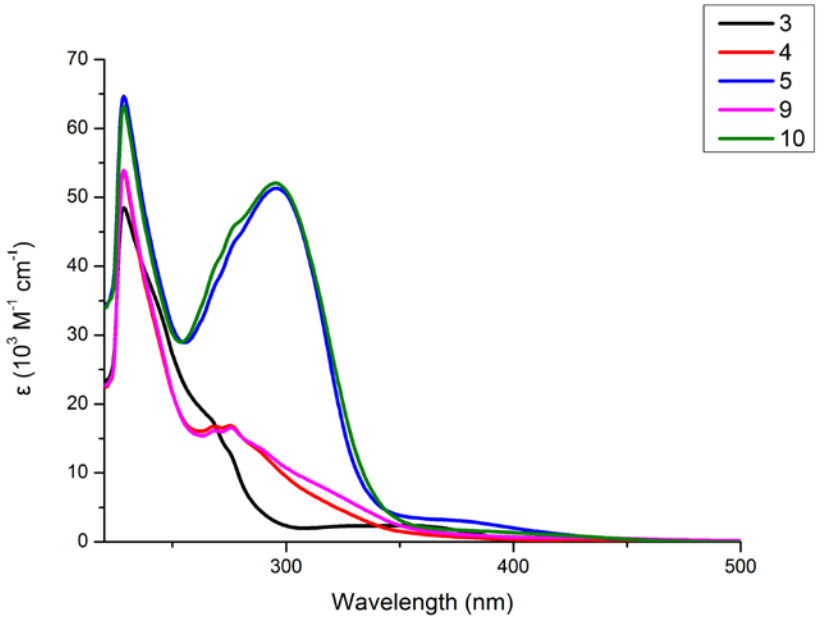

Fig 18. Electronic absorption spectra of complexes 3, 4, 5, 9, 10.

A similar general trend is observed in the electronic absorption spectra of the complexes. Complexes (**1,2,6,7,8**) all show one strong absorption in the UV region and less intense absorptions in the UV region at approximately 200 nm and 267 nm respectively. Complexes (**4,5,9,10**) display two intense absorptions in the UV region at

around 228 and 275 nm. However, complex **3** only exhibited one strong absorption in the UV region at 228 nm and one less intense absorption in the UV region at 267 nm. Based on the intensity and position, the intense absorption in the UV region at 200-229 nm may be attributed to intra-ligand $\pi \rightarrow \pi^*$ transitions.[76] The absorptions in the UV region at 267-295 nm were probably assignable to metal-to-ligand charge transfer transitions (MLCT) band from highest occupied molecular orbital (HOMO) of ruthenium to the vacant π^* orbital of pyridine or pyridyl ligands. From Figure 18, a clear redshifting of the absorption bands is evident between complexes (**4, 9**) and complexes (**5, 10**). This may arise from the stability and enhanced-conjugated system of compounds (**5, 10**) compared to that of compounds (**4, 9**), which substantially stabilize the π^* orbital of the coordinated 4-phenylpyridine ligand. However, the complexes (**4, 9**) possessed a stronger electron acceptor group ($-CO_2Et$) in comparison to the complexes (**5, 10**), which have the 4-phenyl pyridine group ($-C_{11}H_9N$) and should ensure that the MLCT bands of compounds (**4, 9**) are stronger than that of the complexes (**5, 10**).

Based on the weak low energy absorptions, experiments were carried out to investigate the stability of the complexes. However, the results remained the same and demonstrated that weak low energy peaks were not associated with decomposition of the compounds. Moreover, when different solvents were investigated, such as chloroform, the results remained unchanged, which indicated that the solvent had no effect on the absorption behaviour.

Ru(II) complexes of pyridine/pyridyl ligands frequently resulted in MLCT absorptions at relatively low energies(around 300 to 500 nm).[35,36] However, interestingly, it was discovered in this research that there were no prominent peaks in this region. These observations are in agreement with the recent results of our group's DFT (density functional theory) calculations. The results revealed that this type of complex should show only very weak absorptions in the visible or near-UV region.

2.3.4 Electrochemical Studies

The electrochemical properties of compounds (**1-10**) were studied by cyclic voltammetry. The electrochemical data is given in Table 3, while the voltammograms are shown in Fig 19 and Fig 20.

Complexes	E_{pa} (V)	E_{pc} (V)
1	1.2	-0.85
2	1.2	-0.38
3	1.25	-0.32, -1.10
4	1.23	-0.39, -0.95
5	1.13	-0.29, -0.65
6	1.23, 0.77	-0.90
7	1.34,	-0.37
8	1.35	-0.54
9	1.19	-0.75, -0.45
10	1.12	-0.52, -0.85

Table 3. Electrochemical data for complexes 1, 2, 6, 7, 8 in Acetonitrile and complexes 3, 4, 5, 9, 10 in DCM.

Solutions ca. $5x10^{-4}$ M and 0.1 M in NBu_4PF_6; $\Delta E_p = E_{pa} - E_{pc}$ where, E_{pa} and E_{pc} are anodic and cationic potentials, respectively; scan rate: 100 mV S^{-1}.

The cyclic voltammograms of complexes (**1-10**) exhibited an oxidative response between 1.12 and 1.35 V assigned to $Ru^{II/III}$ oxidation, which is irreversible. The lack of a redox transformation of the compounds was possibly due to the π-back-bonding behaviours of the arene ligands. The irreversible reduction peaks could be found from -0.29 to -1.10 V, which are ascribed to the redox process of the bonded ligand. The redox potential of the $Ru^{II/III}$ couple in complexes (**5, 10**) was lower in comparison to the complexes (**4, 9**) which may be due to the electron acceptor group of compounds (**4, 9**) that inhibited oxidisation. It may be assumed that 4-phenyl pyridine is a superior stabiliser of the trivalent state of ruthenium in the 'piano-stool' mode. The changes in oxidation and reduction potentials are attributed to the relative stabilisation of ruthenium (II) over ruthenium (III) due to a combination of the effects of σ and π that

arose from the ligands.[84] In summary, the anticipated ability order of the electron donating groups (−C_5H_4NR, R= CH_3, H, C_6H_5, CO_2Et) should be [−C_5H_4NR, R= CH_3 >H>C_6H_5>CO_2Et]. Therefore, the expected order of $Ru^{III/II}$ potential should increase in reverse order in relation to the electron group's donating ability.

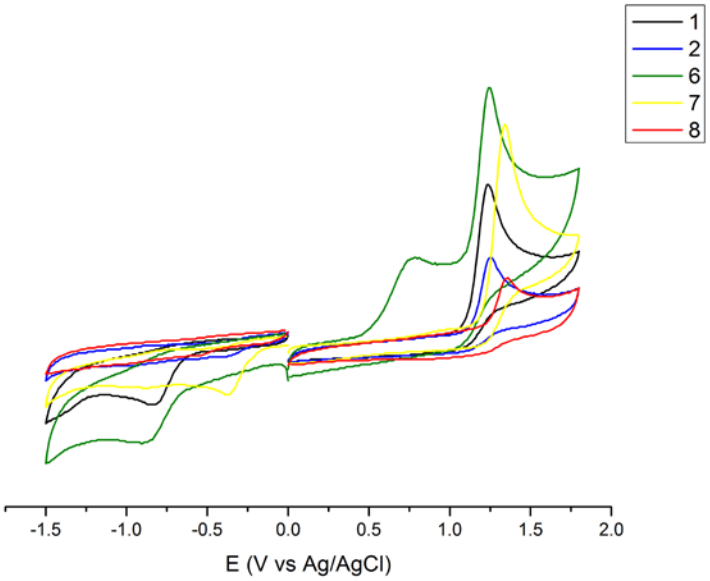

Fig 19. Cyclic voltammograms of complexes (1, 2, 6, 7, 8).

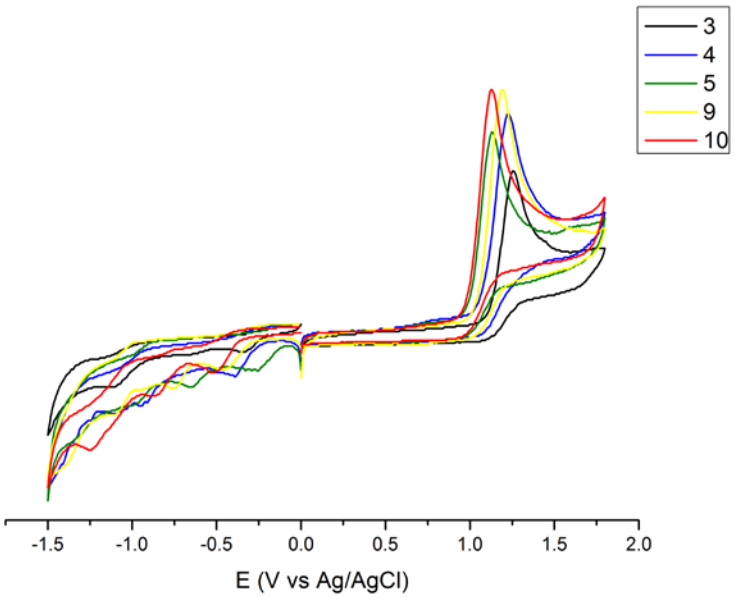

Fig 20. Cyclic voltammograms of complexes (3, 4, 5, 9, 10).

2.3.5 Crystallographic Studies

The crystal structures of $[Ru(Bz)(N_2H_4)_3][BPh_4]_2$ (**1**), $[Ru(Bz)(py)_3][BPh_4]_2$ (**2**), $[Ru(py)_3(DMF)_3][BPh_4]_2$ (**11**), and $[Ru(Cym)(N_2H_4)_3][BPh_4]_2$ (**6**) were obtained, while the molecular structures of the complexes with atom labelling schemes are shown in Figures 21-24. Notably, the counter-anions are not shown. Selected crystallographic data and refinement details for the compounds are presented in Table 4. Selected bond lengths and angles are displayed in Table 5.

Complex salt **1** crystallises in the Cc space group. Meanwhile, the structure reveals the "piano-stool" geometry in Figure 21. From the crystal structure, Ru(II) is coordinated with all six carbon atoms (C1-C6) of the benzene ring and three nitrogen atoms (N1, N3, N5). The N-Ru-N angles range between about 83° and 85°. The six Ru-C bonds are almost the same length, with an average of 2.20(2) Å. The average C-C distance in the planar benzene ring is 1.42(2) Å. The structural features are in good agreement with other reported similar piano-stool compounds.[79, 85]

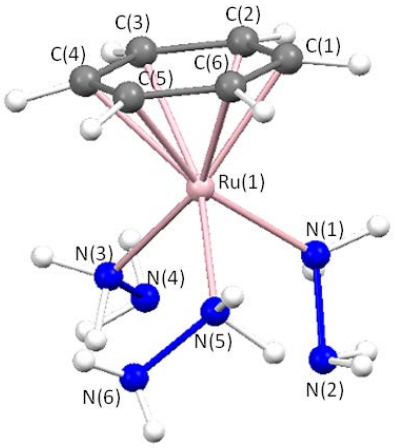

Fig 21. Structural representation of the complex cation in 1.

Complex salt **2** crystallises in the P-1 space group. The entire coordination geometry at the ruthenium atom can be described as the "piano-stool" (Figure 22). The angle of N(2)-Ru(1)-N(3) [96.0(9)°] is larger in comparison to the angles of N(1)-Ru(1)-N(2)

[85.0(9)°] and N(1)-Ru(1)-N(3) [84.2(1)°]. Additionally, the ruthenium atom is bound to the benzene ring with Ru-C average length of 2.197(7) Å.

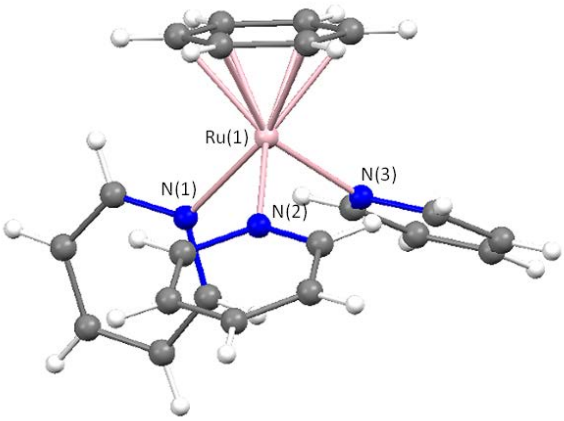

Fig 22. Structural representation of the complex cation in 2.

Complex salt **11** $[Ru(py)_3(DMF)_3][BPh_4]_2$, crystallises in the C2/c space group, which is shown in Figure 23. The angles of N(1)-Ru(1)-N(2), N(1)-Ru(1)-N(3), N(2)-Ru(1)-N(3) are 90.3(3)°, 92.3(2)° and 95.5(9)° respectively. The Ru(1)-N(3) distance [2.182(6) Å] is the same as that in Ru(1)-N(1) [2.182(5) Å] and longer in comparison to Ru(1)-N(2) [2.042(3) Å].

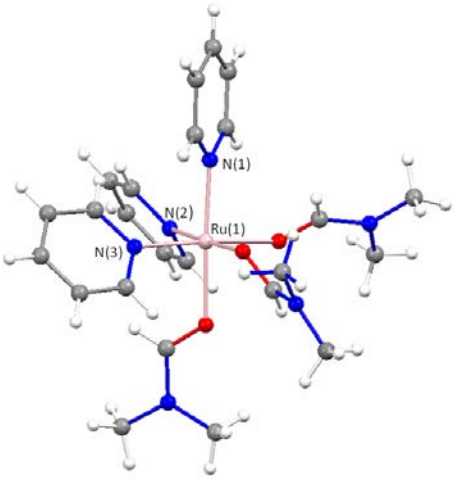

Fig 23. Structural representation of the complex cation in 11.

Complex salt **6** crystallises in the P2(1)/c space group. From Figure 24, the crystal

structure of Ru(II) is coordinated with all six carbon atoms (C1-C6) of the cymene ring and the three nitrogen atoms (N1, N3, N5). The N-Ru-N angles range between about 82° and 88°. The average bond length of Ru-C is 2.203(7) Å. The N_2H_4 ligands exhibit distances of 2.144(2) Å for Ru(1)-N(1) and 2.140(2) Å for Ru(1)-N(5), which are shorter in comparison with Ru(1)-N(3) [2.159(2) Å]. Meanwhile, the average Ru-N distance in **6** [2.148(3) Å] is not significantly different in comparison to **1** [2.129(8) Å].

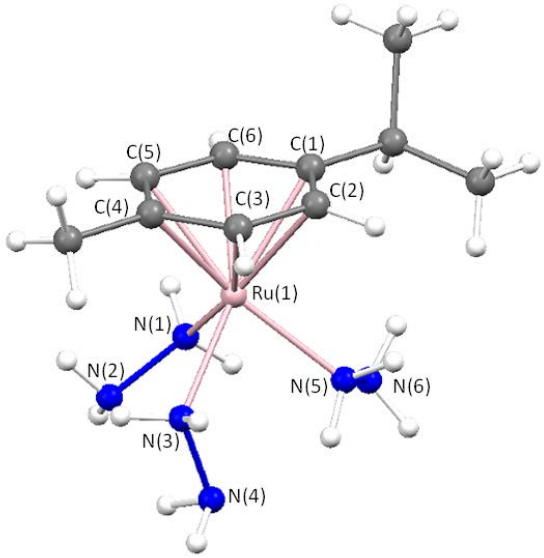

Fig 24. Structural representation of the complex cation in 6.

	1	**2**	**6**	**11**
Empirical formula	$C_{55}\,H_{61}\,B_2\,N_7\,O_2\,Ru$	$C_{72}\,H_{68}\,B_2\,N_4\,O_1\,Ru$	$C_{59}\,H_{69}\,B_2\,N_7\,O_2\,Ru$	$C_{72}\,H_{76}\,B_2\,N_6\,O_3\,Ru$
Formula weight	974.80	1128.08	1030.90	1196.07
Temperature	150(2) K	150(2) K	100(2) K	150 (2) K
Crystal system	Monoclinic	Triclinic	Monoclinic	Monoclinic
Space group	Cc	P-1	P2(1)/c	C2/c
Unit cell dimensions	a = 10.3450(2) Å α = 90° b = 33.9602(5) Å β = 105.9080(10)° c = 14.9685(2) Å γ = 90°	a = 10.9439(5) Å α = 70.327(5)° b = 14.8824(9) Å β = 83.561(4)° c = 18.9340(9) Å γ = 85.819(4)°	a = 18.0440(3) Å α = 90° b = 12.7542(2) Å β = 93.4800(10)° c = 22.2467(4) Å γ = 90°	a = 25.3442(8) Å α = 90° b = 11.1929(3) Å β = 111.692(4)° c = 23.6479(9) Å γ = 90°
Volume	5057.31(14) $Å^3$	2883.5(3) $Å^3$	5057.34(15) $Å^3$	6233.3(4) $Å^3$
Z	4	1	4	4
Absorption coefficient	2.878 mm^{-1}	0.321 mm^{-1}	2.877 mm^{-1}	0.304 mm^{-1}
F(000)	2040	1180	2168	2512
Crystal size	0.26 x 0.17 x 0.07 mm^3	0.20 x 0.20 x 0.22 mm^3	0.14 x 0.12 x 0.04 mm^3	0.40 x 0.30 x 0.20 mm^3
θ range for data collection	4.03 to 72.33°	2.8 to 29.5°	2.45 to 72.15°	5.93 to 50.69°
Reflections collected	13909	21121	47915	16665
Independent reflections	7577 [R(int) = 0.0250]	17028 [R(int) = 0.0378]	10004 [R(int) = 0.0582]	5701 [R(int) = 0.0289]
Goodness-of-fit on F^2	1.110	1.0762	1.029	1.110
Final R indices [$F^2 > 2\sigma(F^2)$]	R1 = 0.0477, wR2 = 0.1343	R1 = 0.0699, wR2 = 0.1638	R1 = 0.0391, wR2 = 0.0978	R1 = 0.0665, wR2 = 0.1628
R indices (all data)	R1 = 0.0489, wR2 = 0.1356	R1 = 0.1048, wR2 = 0.1998	R1 = 0.0484, wR2 = 0.1031	R1 = 0.0734, wR2 = 0.1669
Largest diff. peak and hole	2.287 and -0.522 e.$Å^{-3}$	1.54 and -0.74 e.$Å^{-3}$	2.402 and -0.664 e.$Å^{-3}$	1.56 and -1.17 e.$Å^{-3}$

Table 4. Selected crystallographic data and refinement details for complex salts 1, 2, 6 and 11.

	Ru1-N1	2.132(5)	Ru1-C1	2.198(7)	Ru1-C4	2.206(6)
1	Ru1-N3	2.136(4)	Ru1-C2	2.204(5)	Ru1-C5	2.198(6)
	Ru1-N5	2.118(4)	Ru1-C3	2.216(5)	Ru1-C6	2.186(6)
	N1-Ru1-N3	83.3 (2)	N1-Ru1-N5	85.4(2)	N3-Ru1-N5	85.0(2)
	Ru1-N1	2.125(3)	Ru1-C1	2.192(3)	Ru1-C4	2.202(3)
2	Ru1-N2	2.127(2)	Ru1-C2	2.194(3)	Ru1-C5	2.197(3)
	Ru1-N3	2.146(3)	Ru1-C3	2.203(3)	Ru1-C6	2.196(3)
	N1-Ru1-N2	85.0(9)	N1-Ru1-N3	84.2(1)	N2-Ru1-N3	96.0(9)
	Ru1-N1	2.182(5)	N1-Ru1-N2	90.3(3)		
11	Ru1-N2	2.042(3)	N1-Ru1-N3	92.3(2)		
	Ru1-N3	2.182(6)	N2-Ru1-N3	95.5(9)		
	Ru1-N1	2.144(2)	Ru1-C1	2.212(3)	Ru1-C4	2.236(3)
6	Ru1-N3	2.159(2)	Ru1-C2	2.204(3)	Ru1-C5	2.201(3)
	Ru1-N5	2.140(2)	Ru1-C3	2.201(3)	Ru1-C6	2.167(3)
	N1-Ru1-N3	87.9(8)	N1-Ru1-N5	83.0(1)	N3-Ru1-N5	81.6(1)

Table 5. Selected interatomic distances (Å) and angles (°) for complex salts 1, 2, 6 and 11.

Chapter Three - Piano-Stool Ruthenium (II) Complexes with HMB Ring

3.1 Introduction

Based on the previous work, another immediate research objective is changing the capping ring. The dimeric complex $[Ru^{II}Cl_2(HMB)]_2$ (HMB: hexamethylbenzene) is already known and commercially available. Due to the more stable structure and electron-rich system of hexamethylbenzene, it may ensure that the C_{3v} symmetry is more stable and acts as a superior donor for the D-π-A system. It compares well with the benzene and cymene system.

The literature review revealed that these dimers are widely used as important precursors in the substitution reaction,[86-88] oxidation reactions[89] and for making potential anti-cancer complexes.[90] Two C_{3v} symmetrical complexes $[Ru(HMB)(Cl)_3](CH_2Cl_2)$ and $[Ru(HMB)(CH_3CN)_3](BF_4)_2$ have already been created by Kolle's group[91] and Ramirez-Monroy's group[92] respectively.

3.2 Experimental

3.2.1 Materials and Procedures

All reactions were carried out under a nitrogen atmosphere, and all solvents were degassed using nitrogen. Products were dried at room temperature overnight in a vacuum desiccator (SiO_2). All other reagents were obtained commercially and used as supplied.

3.2.2 General Physical Measurements

Mass spectra were recorded using a Thermo-Quest Finnigan Trace GC/MS or Thermo Electron Finnigan LTQ FT mass spectrometers. MALDI mass spectra were recorded using a micromass/Waters TOF spec 2E instrument. ^{1}H NMR (Nuclear magnetic resonance) spectra were recorded on Bruker Ultrashield 400 MHz and 500 MHz spectrometers, while all chemical shifts were quoted with respect to TMS. The microanalysis was conducted in collaboration with the School of Chemistry at the University of Manchester (UK).

3.2.3 Syntheses

$[Ru(HMB)(N_2H_4)_3][BPh_4]_2$, [12]

A suspension of $[Ru^{II}Cl_2(HMB)]_2$ (200 mg, 0.299 mmol) in THF (10 mL) was added hydrazine hydrate (0.5 mL), and the mixture stirred at room temperature under Ar for 30 min. $NaBPh_4$ (800 mg, 2.34 mmol) was added with stirring to give a pale yellow precipitate which was filtered off, washed with water and dried. Yield: 550 mg, 92%; δ_H (CD_3SOCD_3) 7.18–7.16 (16 H, d, J = 7.2, BPh_4), 6.94–6.90 (16 H, t, J = 7.0, BPh_4),

6.80–6.77 (8 H, t, *J* = 6.8, BPh_4), 5.86 (6 H, s, $3NH_2$), 3.84 (6 H, s, $3NH_2$), 2.08 (18 H, s, 6Me). ES-MS, m/z (-ES): 319.2 ($[BPh4]^-$). m/z (+ES): 330.0 ($[M - N_2H_4]^+$), 295.0 ($[M - 2N_2H_4]^+$). Anal. Calcd (%) for $C_{60}H_{70}B_2N_6Ru \cdot 2.5H_2O$: C, 69.1; H, 7.2; N, 8.1. Found: C, 68.9; H, 7.1; N, 8.8.

$[Ru(HMB)(py)_3][Cl]_2$, [13]

A suspension of $[Ru^{II}Cl_2(HMB)]_2$ (133 mg, 0.20 mmol) was refluxed in ethanol (50 mL). And pyridine (0.10 mL) added. The resulting mixture was refluxed under Ar for 16 h. The mixture was cooled to room temperature and filtered through celite. Then the solution was dried and the crude product precipitated with DCM/Pentane. Yield: 170 mg, 77%; δ_H (DMSO) 8.58 (6H，d, *J* = 3.9, C_5H_5N-$H^{2,6}$), 7.79 (3H，t, *J* = 7.6, C_5H_5N-H^4), 7.46 – 7.34 (6H，m, C_5H_5N-$H^{3,5}$), 2.01 (18H, s, 6Me). ES-MS, m/z (+ES): 338.1 ($[M - C_{12}H_{18}]^+$), 342.1 ($[M - 2C_5H_5N]^+$).

$[Ru(HMB)(pic)_3][Cl]_2$, [14]

A suspension of $[Ru^{II}Cl_2(HMB)]_2$ (133 mg, 0.20 mmol) was refluxed in ethanol (50 mL), and 4-picolline (0.12 mL) added. The resulting mixture was refluxed under Ar for 16 h. And the mixture was cooled to room temperature and filtered through celite. Then the solution wad dried and the crude product precipitated with DCM/Pentane. Yield: 150mg, 63%; δ_H (CD_3CN) 8.57 (6 H, d, *J* = 6.5, C_5H_4N), 7.23 (6 H, d, *J* = 6.0, C_5H_4N), 2.44 (9 H, s, NC_5H_4-C*H*$_3$), 1.98 – 1.96 (18 H, s, 6Me). ES-MS, m/z (+ES)= 356.1 ($[M - 2C_6H_7N]^+$), 380.1 ($[M - C_{12}H_{18}]^+$).

$[Ru(HMB)(ein)_3][Cl]_2$, [15]

A suspension of $[Ru^{II}Cl_2(HMB)]_2$ (133 mg, 0.20 mmol) was refluxed in ethanol (50 mL), and ethyl isonicotinate (0.12 mL) added. The resulting mixture was refluxed under Ar for 16 h. And the mixture was cooled to room temperature and filtered through celite. Then the solution wad dried and the crude product precipitated with

DCM/Pentane. Yield: 200mg, 65%; δ_H (400 MHz, CD_3CN) 8.50 – 8.45 (6 H, m, C_5H_4N), 7.96 – 7.92 (6 H, m，C_5H_4N), 4.36 (6 H, t, *J* = 7.1, OCH_2), 2.16 (18 H, s, 6Me), 1.28 (9 H, t, *J* = 6.8，OCH_2-C*H*$_3$). ES-MS, m/z(+ES)= 454.14 ($[M - Ru - C_{12}H_{18}]^+$), 152.03 ($[M - Ru - C_{12}H_{18} - 2\ C_8H_9NO_2]^+$).

$[Ru(HMB)(ppy)_3][BPh_4]_2$, [16]

To a suspension of $[Ru(HMB)(N_2H_4)_3][BPh_4]_2$ (200 mg, 0.200 mmol) in THF (10 mL) was added 4-phenylpyridine (0.5 mL), and the mixture was stirred at room temperature under Ar for 3 hours. $NaBPh_4$ (800 mg, 2.34 mmol) was added with stirring to give a precipitate which was filtered off, washed with water and dried. Yield: 400mg, 74%; δ_H (Acetone) 8.61 – 8.46 (6 H, m, $C_{11}H_9N$), 7.93 – 7.58 (12 H, m, $C_{11}H_9N$), 7.57 – 7.31 (9 H, m, $C_{11}H_9N$), 7.20 (16 H, d, *J* = 7.2, BPh_4), 6.78 (16 H, t, *J* = 6.8, BPh_4), 6.64 (8 H, t, *J* = 6.7, BPh_4), 2.16 (18 H, s, 6Me). ES-MS, m/z (-ES)= 319.2 ($[BPh4]^-$). m/z(+ES)= 574.2 ($[M - C_{11}H_9N]^+$), 418.1 ($[M - 2C_{11}H_9N]^+$). Anal. Calcd (%) for $C_{91}H_{81}N_3B_2Ru{\cdot}4H_2O$: C, 77.59; H, 6.51; N, 2.91. Found: C, 77.28; H, 5.96; N, 3.22. TGA indicates the loss of ca. 4 molecules of water from the compound upon heating.

3.2.4 X-Ray Crystallography

A crystal of $[Ru(HMB)(N_2H_4)_3][BPh_4]_2$ was obtained by slow diffusion of dichloromethane/pentane. Three other unexpected crystals of $[Ru(HMB)(py)(Cl)_2]$ (**17**), $[Ru(HMB)(pic)(Cl)_2]$ (**18**) and $[Ru(HMB)(pic)(Cl)_2]{\bullet}CH_2Cl_2$ (**19**) were also obtained accidentally by slow vapour diffusion of dichloromethane/pentane according to the same solvent system of $[Ru(HMB)(N_2H_4)_3][BPh_4]_2$. Dr J. Raftery solved all crystal structures at The University of Manchester.

3.3 Results and Discussion

3.3.1 Synthetic Characterization Studies

Based on the previous synthetic method and the literature, the synthesis of $[Ru(HMB)(N_2H_4)_3][BPh_4]_2$ was successful. However, when the same approach was applied to make other HMB ruthenium piano stool complexes, they all failed except $[Ru(HMB)(ppy)_3][BPh_4]_2$.

One reported study by Gras's group[93] revealed that the similar compound $[Ru(HMB)(SC_5H_4NH)_3][Cl]_2$ was also made successfully. The method mentioned involves a reflux system combined with ethanol. Therefore, by modifying this approach, a breakthrough was created and ($[Ru(HMB)(py)_3][Cl]_2$, $[Ru(HMB)(pic)_3][Cl]_2$, $[Ru(HMB)(ein)_3][Cl]_2$) compounds were successfully synthesised; the synthetic steps are shown below (See Scheme 2).

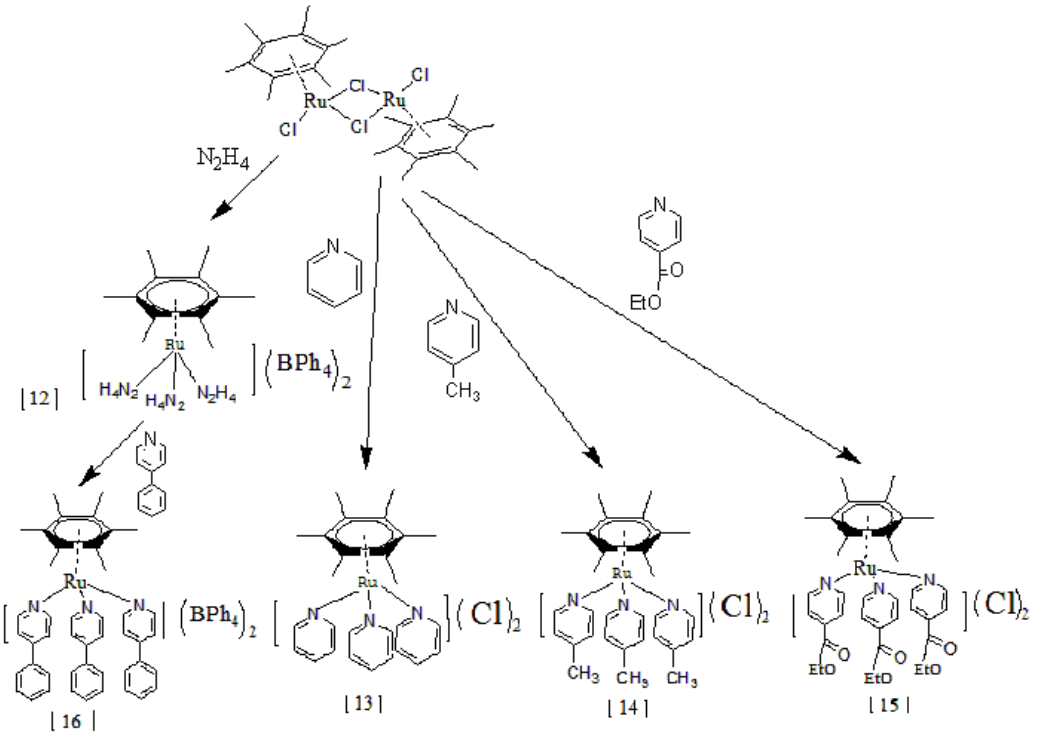

Scheme 2. Synthetic steps.

For compounds (**12**, **16**), the NMR spectra indicated that they were highly pure. Meanwhile, the electrospray mass spectra revealed the existence of complexes and the elemental analyses were consistent with the composition proposed for the complexes. TGA meanwhile indicated the loss of around four molecules of water upon heating for **16**.

For compounds **(13-15)**, the new method was successful. However, the NMR data showed that the complexes were not sufficiently pure; several minor peaks were evident. Meanwhile, the electrospray mass spectrum revealed the existence of complexes. Different purification methods such as column chromatography and anion change were trialed, but the purity and microanalysis results remained unchanged.

In summary, the reaction of $[Ru^{II}Cl_2(HMB)]_2$ with hydrazine hydrate or the reaction of $[Ru(HMB)(N_2H_4)_3][BPh_4]_2$ with 4-phenylpyridine in THF at room temperature lead to the formation of novel arene ruthenium piano-stool complexes **(12, 16)**. The reflux reaction of $[Ru^{II}Cl_2(HMB)]_2$ with pyridine or pyridyl ligands in ethanol resulted in the formation of compounds **(13-15)**, although several still contained impurities. Compounds **(12-16)** were all stable in air and were soluble in polar solvents such as acetone and dichloromethane. However, they were insoluble in diethyl ether and pentane. Meanwhile, the diamagnetic nature of all complexes was consistent with the +2 oxidation state.

3.3.2 ^{1}H NMR Spectroscopy Studies

The ^{1}H NMR spectra of all complexes were well defined when recorded in deuterated CD_3SOCD_3 (dimethylsulfoxide-d_6) or DMSO or CD_3CN or acetone solution to probe the solution structure (Table 6). A representative spectrum is shown in Figure 25.

Complexes	^{1}H NMR data (ppm, J in Hz)
12	7.18–7.16 (16 H, d, *J* = 7.2, BPh_4), 6.94–6.90 (16 H, t, *J* = 7.0, BPh_4), 6.80–6.77 (8 H, t, *J* = 6.8, BPh_4), 5.86 (6 H, s, $3NH_2$), 3.84 (6 H, s, $3NH_2$), 2.08 (18 H, s, 6Me)
13	8.58 (6H， d, *J* = 3.9, C_5H_5N-$H^{2,6}$), 7.79 (3H， t, *J* = 7.6, C_5H_5N-H^{4}), 7.46 – 7.34 (6H， m, C_5H_5N-$H^{3,5}$), 2.01 (18H, s, 6Me)
14	8.57 (6 H, d, *J* = 6.5, C_5H_4N), 7.23 (6 H, d, *J* = 6.0, C_5H_4N), 2.44 (9 H, s, NC_5H_4-C*H*$_3$), 1.98 – 1.96 (18 H, s, 6Me)
15	8.50 – 8.45 (6 H, m， C_5H_4N), 7.96 – 7.92 (6 H, m， C_5H_4N), 4.36 (6 H, t, *J* = 7.1, OCH_2), 2.16 (18 H, s, 6Me), 1.28 (9 H, t, *J* = 6.8， OCH_2-C*H*$_3$)
16	8.61 – 8.46 (6 H, m, $C_{11}H_9N$), 7.93 – 7.58 (12 H, m, $C_{11}H_9N$), 7.57 – 7.31 (9 H, m, $C_{11}H_9N$), 7.20 (16 H, d, *J* = 7.2, BPh_4), 6.78 (16 H, t, *J* = 6.8, BPh_4), 6.64 (8 H, t, *J* = 6.7, BPh_4), 2.16 (18 H, s, 6Me)

Table 6. Selected ^{1}H NMR data of complexes [12-16].

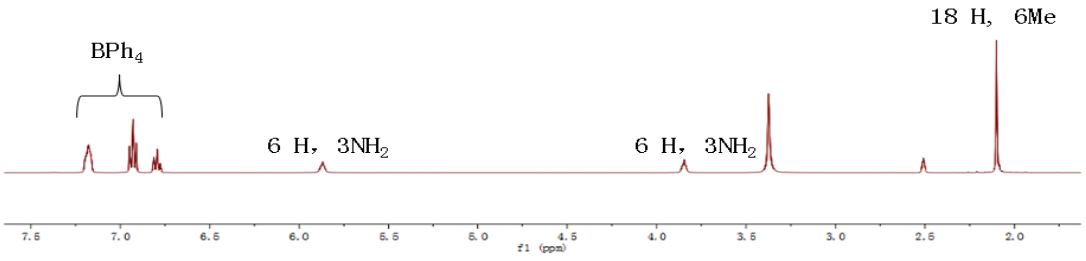

Fig 25. ^{1}H NMR spectrum (deuterated DMSO, 400MHz, room temperature) of 12 $[Ru(HMB)(N_2H_4)_3][BPh_4]_2$.

The compounds **(12, 16)** show three peaks between δ 8 ppm and δ 6 ppm for the presence of BPh_4^-. The protons of the HMB ring of compounds **(12-16)** appeared as singlets around δ 2 ppm. The protons of pyridine or pyridyl ligands represented peaks at around δ 8-7 ppm. The NMR data defined an upfield chemical shift of the ring hydrogen that belonged to the HMB moiety in comparison with the benzene or p-cymene moiety due to the π-back bonding of the ligand to ruthenium. The electron density of ruthenium moved to the HMB ring, which leads to stronger shielding of ring hydrogens.

3.3.3 Crystallographic Studies

The crystal structures of $[Ru(HMB)(N_2H_4)_3][BPh_4]_2$ (**12**), $[Ru(HMB)(py)(Cl)_2]$ (**17**), $[Ru(HMB)(pic)(Cl)_2]$ (**18**), $[Ru(HMB)(pic)(Cl)_2]\bullet CH_2Cl_2$ (**19**) were obtained and the structural representation of the complexes are shown in Figures 26-29. Selected crystallographic data and refinement details for the complexes are shown in Table 7. Meanwhile, selected bond lengths and angles are displayed in Table 8.

Complex salt **12** crystallises in the P-1 space group. From Figure 26, the crystal structure of Ru(II) is coordinated to all six carbon atoms (C1-C6) of the HMB ring and the three nitrogen atoms (N1, N3, N5). The N(1)-Ru(1)-N(5) angle [83.1(8)] is same as N(3)-Ru(1)-N(5) [83.5(1)]. However, both angles are smaller in comparison to N(1)-Ru(1)-N(3) [86.4(8)]. The distances Ru(1)-N(1) [2.147(2) Å], Ru(1)-N(3) [2.143(3) Å] and Ru(1)-N(5) [2.148(2) Å] are effectively the same. The average Ru-C bond lengths in complex salt **6 [**2.203(7) Å] and **12 [**2.207(7) Å] are almost identical, and marginally shorter than that of 2.250(7) Å as reported for $[Ru(HMB)(SC_5H_4NH)_3][Cl]_2$.[93]

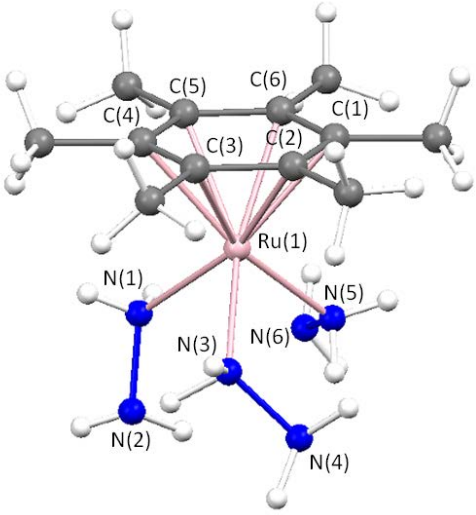

Fig 26. Structural representation of the complex cation in 12.

Complex **17** crystallises in the P-1 space group. The entire coordination geometry at the

ruthenium atom can be described as “piano-stool”. From Figure 27, the bond distance of Ru(1)-Cl(1) [2.418(5) Å] and Ru(1)-Cl(2) [2.422(5) Å] are not significantly different. Meanwhile, the angles N(1)-Ru-Cl(1) and N(1)-Ru(1)-Cl(2) are 86.10(4)° and 85.12(5)° respectively. The angle Cl(1)-Ru(1)-Cl(2) is 89.26(2)°. The six Ru-C bonds are almost the same length, with an average of 2.20(5) Å.

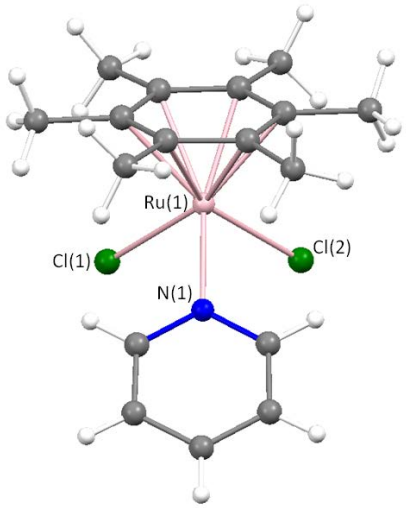

Fig 27. Structural representation of the complex 17.

Complex **18** crystallises in the P2(1)/n space group. From Figure 28, the bond distance of Ru(1)-N(1) is 2.13(2) Å and the Cl(1)-Ru(1)-Cl(2) angle is 88.5(2)°, moreover N(1)-Ru(1)-Cl(1) angle [86.04(5)°] is close to N(1)-Ru(1)-Cl(2) angle [85.74(5)°]. Meanwhile, the average ruthenium to carbon distance is 2.201(5) Å.

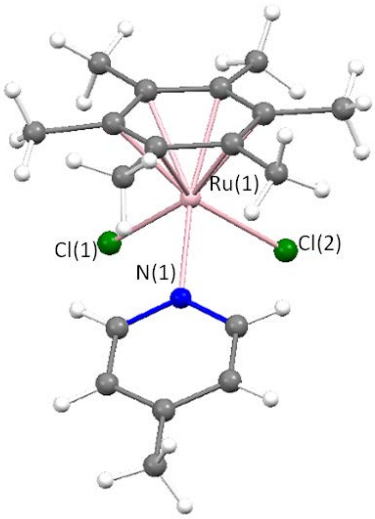

Fig 28. Structural representation of the complex 18.

Complex **19** crystallises in the Iba2 space group. (Figure 29) The Ru(1)-Cl(1) distance [2.410(6) Å] is similar to the Ru(1)-Cl(2) distance [2.419(7) Å]. The N(1)-Ru(1)-Cl(1) angle, N(1)-Ru(1)-Cl(2) angle and Cl(1)-Ru(1)-Cl(2) angle are arranged in the following order 85.93(6)°, 86.29(6)°, 87.56(2)°. The average bond length of Ru-C is 2.205(6) Å.

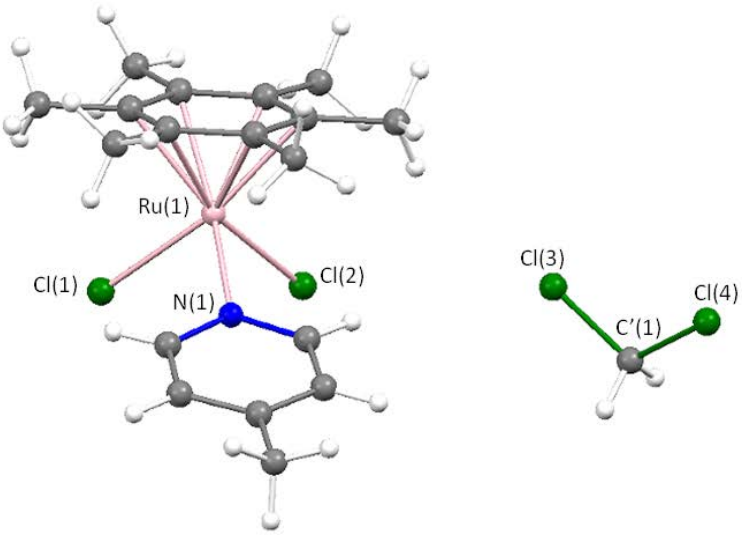

Fig 29. Structural representation of the complex 19.

	12	**17**	**18**	**19**
Empirical formula	$C_{61}\,H_{73}\,B_2\,N_7\,O_2\,Ru$	$C_{17}\,H_{23}\,Cl_2\,N\,Ru$	$C_{18}\,H_{25}\,Cl_2\,N\,Ru$	$C_{18.5}\,H_{26}\,Cl_3\,N\,Ru$
Formula weight	1058.95	413.33	427.36	469.82
Temperature	100(2) K	100(2) K	100(2) K	100 (2) K
Crystal system	Triclinic	Triclinic	Monoclinic	Orthorhombic
Space group	P-1	P-1	P2(1)/n	Iba2
Unit cell dimensions	a = 12.2122(6) Å α = 69.889(3)° b = 13.2514(6) Å β = 88.286(3)° c = 17.8491(9) Å γ = 87.406(3)°	a = 7.1382(3) Å α = 62.2580(10)° b = 15.8208(7) Å β = 86.539(2)° c = 16.3629(7) Å γ = 84.815(2)°	a = 8.9817(4) Å α = 90° b = 12.4170(5) Å β = 102.263(2)° c = 15.7443(6) Å γ = 90°	a = 16.7321(3) Å α = 90° b = 17.8092(3) Å β = 90° c = 13.1859(3) Å γ = 90°
Volume	2709.3(2) $Å^3$	1628.44(12) $Å^3$	1715.83(12) $Å^3$	3929.21(13) $Å^3$
Z	2	4	4	8
Absorption coefficient	2.726 mm^{-1}	10.733 mm^{-1}	10.208 mm^{-1}	10.195 mm^{-1}
F(000)	1116	840	872	1912
Crystal size	0.24 x 0.16 x 0.08 mm^3	0.19 x 0.14 x 0.03 mm^3	0.17 x 0.14 x 0.09 mm^3	0.29 x 0.07 x 0.04 mm^3
θ range for data collection	2.64 to 72.27°	5.32 to 72.19°	4.58 to 72.40°	3.62 to 72.01°
Reflections collected	21735	19213	11614	8976
Independent reflections	10070 [R(int) = 0.0383]	6197 [R(int) = 0.0221]	3304 [R(int) = 0.0291]	2876 [R(int) = 0.0231]
Goodness-of-fit on F^2	1.046	1.030	1.055	1.075
Final R indices [$F^2 > 2\sigma(F^2)$]	R1 = 0.0394, wR2 = 0.0973	R1 = 0.0192, wR2 = 0.0467	R1 = 0.0214, wR2 = 0.0530	R1 = 0.0191, wR2 = 0.0442
R indices (all data)	R1 = 0.0451, wR2 = 0.1006	R1 = 0.0206, wR2 = 0.0473	R1 = 0.0239, wR2 = 0.0504	R1 = 0.0199, wR2 = 0.0444
Largest diff. peak and hole	1.200 and -0.829 e.$Å^{-3}$	0.407 and -0.353 e.$Å^{-3}$	0.491 and -0.521 e.$Å^{-3}$	0.383 and -0.540 e.$Å^{-3}$

Table 7. Selected crystallographic data and refinement details for compounds 12, 17, 18 and 19.

	Ru1-N1	2.147(2)	Ru1-C1	2.219(3)	Ru1-C4	2.195(3)
12	Ru1-N3	2.143(3)	Ru1-C2	2.212(2)	Ru1-C5	2.198(3)
	Ru1-N5	2.148(2)	Ru1-C3	2.217(2)	Ru1-C6	2.202(3)
	N1-Ru1-N3	86.4(8)	N1-Ru1-N5	83.1 (8)	N3-Ru1-N5	83.5(1)
	Ru1-N1	2.13(2)	Ru1-C1	2.20(2)	Ru1-C4	2.20(2)
17	Ru1-Cl1	2.418(5)	Ru1-C2	2.19(2)	Ru1-C5	2.20(2)
	Ru1-Cl2	2.422(5)	Ru1-C3	2.21(2)	Ru1-C6	2.20(2)
	N1-Ru1-Cl1	86.10(4)	N1-Ru1-Cl2	85.12(5)	Cl1-Ru1-Cl2	89.26 (2)
	Ru1-N1	2.13(2)	Ru1-C1	2.207(2)	Ru1-C4	2.194(2)
18	Ru1-Cl1	2.412(5)	Ru1-C2	2.179(2)	Ru1-C5	2.205(2)
	Ru1-Cl2	2.411(5)	Ru1-C3	2.216(2)	Ru1-C6	2.205(2)
	N1-Ru1-Cl1	86.0(4)	N1-Ru1-Cl2	85.7(4)	Cl1-Ru1-Cl2	88.5(2)
	Ru1-N1	2.121(2)	Ru1-C1	2.216(2)	Ru1-C4	2.194(3)
19	Ru1-Cl1	2.410(6)	Ru1-C2	2.200(3)	Ru1-C5	2.206(2)
	Ru1-Cl2	2.419(7)	Ru1-C3	2.212(3)	Ru1-C6	2.201(2)
	C’(1)-Cl3	1.761(3)	C’(1)-Cl4	1.761(3)		
	N1-Ru1-Cl1	85.93(6)	N1-Ru1-Cl2	86.29(6)	Cl1-Ru1-Cl2	87.56(2)
	Cl3-C’(1)-Cl4	112.0(3)				

Table 8. Selected interatomic distances (Å) and angles (°) for compounds 12, 17, 18 and 19.

Chapter Four Conclusions

As a precursor for NLO studies with functionalised complexes, basic coordination chemistry with simple ligands has been studied, which is related to Ru(II) tris-pyridyl complexes with a capping benzene, cymene or hexamethylbenzene ring. The compounds $[Ru(Bz)(N_2H_4)_3][BPh_4]_2$ (**1**), $[Ru(Cym)(N_2H_4)_3][BPh_4]_2$ (**6**) and $[Ru(HMB)(N_2H_4)_3][BPh_4]_2$ (**12**) were first synthesized using commercially available dimers and then used as precursors to generate a series of piano-stool ruthenium (II) complexes with pyridine or pyridyl ligands. The complex salts prepared included $[Ru(Bz)(py)_3][BPh_4]_2$ (**2**), $[Ru(Cym)(py)_3][BPh_4]_2$ (**7**) and $[Ru(HMB)(ppy)_3][BPh_4]_2$ (**16**). Interestingly, electronic spectroscopy studies revealed only very weak absorptions in the 300 to 500 nm region. Furthermore, the recent DFT studies by our group confirmed that these experimental observations were consistent with the weak absorptions of electronic spectroscopy studies. The electrochemical studies also reinforced a theory that the redox process of compounds was irreversible. Trials with column purification, as well as exposing the products to air, demonstrated the stability order of the complexes as being arene= HMB > cymene > benzene. Therefore, the ruthenium benzene compounds were the most unstable among them. Moreover eight interesting novel crystal structures (compounds = **1**, **2**, **6**, **11**, **12**, **17**, **18, 19**) were also obtained. Notably, compound **11** $[Ru(py)_3(DMF)_3][BPh_4]_2$ was found when complex **2** $[Ru(Bz)(py)_3][BPh_4]_2$ decomposed in the solvent system DMF/diethyl ether.

Chapter Five Future Work

In the present study, twelve novel complexes have been successfully fabricated. The first aim of this study was to synthesise of a series of new C_{3v} chromophores and characterise them by experimental and theoretical methods; significant progress was made but further research is required. The electronic spectroscopy results showed unexpectedly weak absorption at low energies, which could be assumed to lead to a small first hyperpolarisability (second-order) β. Meanwhile, the irreversible redox properties of compounds ensure that the reversible redox switching of β becomes impossible. Notably, the stability of the compounds will also have an influence on making LB films as well. It may be feasible to replace the 'piano-stool' ligands with long chain ligands. However, the issues of purification and stability may become quite substantial according to the prior purification and synthesis experience.

Beyond the research presented in this study, the next step will include replacing the current pyridyl ligands with long chain pyridinium-substituted ligands. Although the purification is likely to prove challenging, it is still worth trialing in order to make these novel complexes. Alternatively, the ring of the 'piano-stool' compounds could also be altered. For example, the cyclopentadienyl ring could be trialed. If these compounds are successfully fabricated, the β switching properties of these complexes may be feasible and the stability may also change. In this case, making LB films will become more viable. Finally, the combination of an anionic capping ligand with pyridyl derivatives bearing electron-withdrawing substituents may lead to new complexes with large and switchable NLO responses.

References

1. Nonlinear Optical Properties of Matter: From Molecules to Condensed Phase (Eds: M G Papadopoulos et al.), Springer, Dordrecht, 2006.
2. C. Chen, Z. G. Lin, Ann Rev. Mat. Sci, 1986, **16**, 203.
3. B. J. Coe, in Comprehensive Coordination Chemistry II, Elsevier Pergamon, Oxford, 2004; Vol. **9**, 621; D. S. Bella, C. Dragonetti, M. Pizzotti, D. Roberto, F. Tessore, R. Ugo, *Top. Organomet. Chem*, 2010, **28**, 1; O. Maury, H. Le Bozec, in Molecular Materials, Wiley, Chichester, 2010, 1.
4. B. J. Coe, N. R. M Curati, Comments. Inorg. Chem, 2004, **25**, 147; P. J. Low, Dalton. Trans, 2005, 2821.
5. B. J. Coe, Chem. Eur. J, 1999, **5**, 2464; I. Asselberghs, K. Clays, A. Persoons, D. M. Ward, J. Mccleverty, J. Mater. Chem, 2004, **14**, 2831.
6. H. M. Green M, R. S. Marder, E. M. Thompson, A. J. Bandy, D. Bloor, V. P. Kolinsky, J. R. Jones, Nature, 1987, **330**, 360.
7. C. B. Rinderspacher, W. J. Andzelm, M. A. Rawlett, M. J. Dougherty, M. Baranoski, C. M. Davis, Chem. Phys. Lett, 2011, **507**, 221.
8. A. Valore , A. Colombo, C. Dragonetti, S. Righetto, D. Roberto, R. Ugo, D. F. Angelis, S. Fantacci, Chem. Commun, 2010, **46**, 2414.
9. Q. Li, K. Wu, Q. Y. Wei, R. Sa, Y. Cui, C. Lu, J. Zhu, J. He, Phys. Chem. Chem. Phys, 2009, **11**, 4490.
10. L. Serrano-Andrés, A. Avramopoulos, J. Li, P. Labéguerie, D. Bégué, V. Kellö, G. M. Papadopoulos, J. Chem. Phys, 2009, **131**, 134312.
11. M. Pizzotti, R. Ugo , C. Dragonetti, E. Annoni, Organometallics, 2003, **22**, 4001.
12. P. Kaur, M. Kaur, G. Depotter, V. S. Cleuvenbergen, I. Asselberghs, K. Clays, K. Singh, J. Mater. Chem, 2012, **22**, 10597.
13. V. S. Cleuvenbergen, I. Asselberghs, M. E. García-Frutos, B. Gómez-Lor, K. Clays, J. Perez-Moreno, J. Phys. Chem. C, 2012, **116**, 12312.
14. N. Jiang, G. Zuber, S. Keinan, A. Nayak, W. Yang, J. M. Therien, N. D. Beratan, J.

Phys. Chem. C, 2012, **116**, 9724.

15. Y. Z. Liu, Y. G. Lu, J. Ma, J. Phys. Org. Chem, 2011, **24**, 568.
16. P. Hrobárik, I. Sigmundová, P. Zahradník, P. Kasak, V. Arion, E. Franz, K. Clays, J. Phys. Chem. C, 2010, **114**, 22289.
17. C. Zhang , H. Cao, C. Im, G. Lu, J. Phys. Chem. A, 2009, **113**, 12295.
18. S. Houbrechts, K. Clays, A. Persoons, V. Cadierno, P. M. Gamasa, J. Gimeno, Organometallics, 1996, **15**, 5266.
19. N. Nemoto, J. Abe, F. Miyata, Y. Shirai, Y. Nagase, J. Mater. Chem, 1997, **7**, 1389.
20. B. Ruiz, M. Jazbinsek, P. Günter, Cryst. Growth Des, 2008, **8**, 4021.
21. K. Jagannathan, S. Kalainathan, T. Gnanasekaran, N. Vijayan, G. Bhagavannarayana, Cryst. Growth Des, 2007, **7**, 1881.
22. S. Brahadeeswaran, S. Onduka, M. Takagi, Y. Takahashi, H. Adachi, T. Kamimura, M. Yoshimura, Y. Mori, K. Yoshida, T. Sasaki, Cryst. Growth Des, 2006, **6,** 2463.
23. J. R. Morris, F. W. Stanislaw, J. Org. Chem, 1993, **58**, 3800.
24. B. Ruiz, Z. Yang, V. Gramlich, M. Jazbinsek, P. Günter, J. Mater. Chem, 2006, **16**, 2839.
25. Z. Yang, M. Jazbinsek, B. Ruiz, S. Aravazhi, V. Gramlich, P. Günter, Chem. Mater, 2007, **19**, 3512.
26. Z. Yang, L. Mutter, B. Ruiz, S. Aravazhi, M. Stillhart, M. Jazbinsek, V. Gramlich, P. Gunter, Adv. Funct. Mater, 2007, **17**, 2018.
27. S. Okada, A. Masaki, H. Matsuda, H. Nakanishi, M. Kato, R. Muramatsu, M. Otsuka, 1990, Jpn. J. Appl. Phys, **29**, 1112.
28. N. C. Nishimura, X. Duan, K. Komatsu, S. Okada, H. Oikawa, H. Matsuda, H. Nakanishi, Nonlinear. Opt, 1999, **22**, 247.
29. T. Matsukawa, Y. Takahashi, R. Miyabara, H. Koga, H. Umezawa, I. Kawayama, M. Yoshimura, S. Okada, M. Tonouchi, Y. Kitaoka, Y. Mori, T. Sasaki, 2009, J. Cryst. Growth, **311**, 568.
30. H. Figi, L. Mutter, C. Hunziker, M. Jazbinsek, P. Günter, B. J. Coe, J. Opt. Soc. Am, 2008, B **25**, 1786.
31. S. Zrig, G. Koeckelberghs, T. Verbiest, B. Andrioletti, E. Rose, A. Persoons, I.

Asselberghs, K. Clays, J. Org. Chem, 2007, **72**, 5855; C.-G. Liu, Y.-Q. Qiu, Z.-M. Su, G.-C. Yang, S.-L. Sun, J. Phys. Chem. C, 2008, **112**, 7021; H.-P. Li , K. Han, G. Tang, M.-X. Li, X.-P. Shen, Z.-M. Huang, Mol. Phys, 2009, **107**, 1597; S. Sergeyev, D. Didier, V. Boitsov, A. Teshome, I. Asselberghs, K. Clays, L. C. Vande Velde, A. Plaquet, B. Champagne, Chem. Eur. J, 2010, **16**, 8181.

32. Y. Liu, X. Xu, T. Zheng, Y. Cui, Angew. Chem. Int. Ed, 2008, **47**, 4538; J. Campo, A. Painelli, F. Terenziani, V. T. Regemorter, D. Beljonne, E. Goovaerts, W. Wenseleers, J. Am. Chem. Soc, 2010, **132**, 16467; T. lshizuka, E. L. Sinks, K. Song, S-T. Hung, A. Nayak, K. Clays, J. M. Therien, J. Am. Chem. Soc, 2011, **133**, 2884; M-Y. Jeong, S. Brasselet, T-K. Lim, B. Raecho, Adv. Funct. Mater, 2012, **22**, 788.
33. (a) O. Maury, L. Viau, K. Senechal, B. Corre, J. Guegan, T. Renouard, I. Ledoux, J. Zyss, L. H. Bozec, Chem. Eur. J, 2004, **10**, 4454; (b) B. J. Coe, J. A. Harris, B. S. Brunschwig, I. Asselberghs, K. Clays, J.Garin, J. Orduna, J. Am. Chem. Soc, 2005, **127**, 13399; (c) O. Maury, H. Le Bozec, Acc. Chem. Res, 2005, **38**, 691; (d) S. Bidault, S. Brasselet, J. Zyss, O. Maury, L. H. Bozec, J. Chem. Phys, 2007, **126**, 034312-1; (e) B. J. Coe, J. Fielden, SP. Foxon, BS. Brunschwig, I. Asselberghs, K. Clays, A. Samoc & M. Samoc, J. Am. Chem. Soc, 2010, **132**, 3496.
34. E. M. Maya, E. M. Garcia-Frutos, P. Vázquez, T. Torres, G. Martín, G. Rojo, F. Agulló-López, H. R. González-Jonte, R. V. Ferro, J. M. G. de La Vega, I. Ledoux, J. Zyss, J. Phys. Chem A, 2003, **107**, 2110; L. Rigamonti, F. Demartin, A. Forni, S. Righetto, A. Pasini, Inorg. Chem, 2006, **45**, 10976; J. Tedim, S. Patricio, R. Bessada, R. Morais, C. Sousa, B. M. Marques, C. Freire, Eur. J. Inorg Chem, 2006, 3425; S. Di Bella, P. I. Oliveri, A. Colombo, C. Dragonetti, S. Righetto, D. Roberto, Dalton. Trans, 2012, **41**, 7013.
35. B. J. Coe, J. A. Harris, L. A. Jones, B. S. Brunschwig, K. Song, K. Clays, J. Garín, J. Orduna, S. J. Coles, M. B. Hursthouse, J. Am. Chem. Soc, 2005, **127**, 4845; B. J. Coe, S. P. Foxon, E. C. Harper, M. Helliwell, J. Raftery, C. A. Swanson, B.S. Brunschwig, K. Clays, E. Franz, J. Garín, J. Orduna, P. N. Horton, M. B. Hursthouse, J. Am. Chem. Soc, 2010, **132**, 1706.
36. B. J. Coe, J. Fielden, S. P. Foxon, I. Asselberghs, K. Clays, B. S. Brunschwig, Inorg.

Chem, 2010, **49**, 10718.

37. B. J. Coe, L. J. Harris, M. Helliwell, A. L. Jones, I. Asselberghs, K. Clays, B. Brunschwig, A. J. Harris, J. Garin, J. Orduna, J. Am. Chem. Soc, 2006, **128**, 12192.
38. K. S. Hurst, P. M. Cifuentes, L. P. J. Morrall, T. N. Lucas, R. I. Whittall, G. M. Humphrey, I. Asselberghs, A. Persoons, M. Samoc, B. Luther-Davies, C. A. Willis, Organometallics, 2001, **20**, 4664.
39. X-X. Sun, G-C. Yang, S-L. Sun, N-N. Ma, Y-Q. Qiu, J. Organomet. Chem, 2011, **696**, 3384.
40. T. G. Dalton, P. M. Cifuentes, S. Petrie, R. Stranger, M. G. Humphrey, M. Samoc, J. Am. Chem. Soc, 2007, **129**, 11882.
41. G. C. Liu, H. X. Guan, Phys. Chem. Chem. Phys, 2012, **14**, 5297.
42. L. Ordronneau, H. Nitadori, I. Ledoux, A. Singh, J. A. G. Williams, M. Akita, V. Guerchais, H. Le Bozec, Inorg. Chem, 2012, **51**, 5627.
43. B. Champagne, A. Plaquet, J.-L. Pozzo, V. Rodriguez, F. Castet, J. Am. Chem. Soc, 2012, **134**, 8101.
44. E. Hendrickx, K. Clays, A. Persoons, C. Dehu, J. Bredas, J. Am. Chem. Soc, 1995, **117**, 3547; R. Loucif-Saibi, K. Nakatani, J. A. Delaire, M. Dumont, Z. Sekkat, Chem. Mater, 1993, **5**, 229; S. L. Gilat, S. H. Kawai, J. Lehn, Chem. Eur. J, 1995, **1**, 275; S. Houbrechts, K. Clays, A. Pearsoons, Z. Pikramenou, J. Lehn, Chem. Phys. Lett, 1996, **258**, 485; K. Nakatani, J. A. Delaire, Chem. Mater, 1997, **9**, 2682.
45. K. Clays, A. Persoons, Phys. Rev. Lett, 1991, **66**, 2980; K. Clays, A. Persoons, Rev. Sci. Instrum, 1992, **63**, 3285.
46. B. J. Coe, Chem. Eur. J, 1999, **5**, 2464.
47. S. Sortino, S. Petralia, S. Conoci, D. S. Bella, J. Am. Chem. Soc, 2003, **125**, 1122.
48. A. D. Shukla, A. Das, M. E. van der Boom, Angew. Chem. Int. Ed, 2005, **44**, 3237.
49. P. Serra-Crespo, M. A. van der Veen, E. Gobechiya, K. Houthoofd, Y. Filinchuk, C. E. A. Kirschhock, J. A. Martens, B. F. Sels, D. E. De Vos, F. Kapteijn, J. Gascon, J. Am. Chem. Soc, 2012, **134**, 8314.
50. B. Champagne, A. Plaquet, J-L. Pozzo, V. Rodriguez, F. Castet, J. Am. Chem. Soc, 2012, **134**, 8101.

51. G. D. Torre, G. de la Torre, P. Vázquez, F. Agulló-López, T. Torres, Chem. Rev. 2004, **104**, 3723 and refs therein.
52. C. Lambert, E. Schmälzlin, K. Meerholz, C. Bräuchle, Chem. Eur. J, 1998, **4**, 512; M-H. Ha-Thi, V. Souchon, A. Hamdi, R. Metivier, V. Alain, K. Nakatani, P. G. Lacroix, J-P. Genet, V. Michelet, I. Leray, Chem. Eur. J, 2006, **12**, 9056.
53. I. S. Lee, Y. K. Chung, Inorg. Chem. Commun, 2007, **10**, 593.
54. B. J. Coe, D. Rusanova, results to be published.
55. B. J. Coe, Acc. Chem. Res, 2006, **39**, 383.
56. E. Hendrickx, K. Clays, A. Persoons, Acc. Chem. Res, 1998, **31**, 675.
57. M. Malaun, ZR. Reeves, RL. Paul, JC. Jeffery, JA. McCleverty, MD. Ward, I. Asselberghs, K. Clays, A. Persoons, Chem. Commun, 2001, 49; I. Asselberghs, K. Clays, A. Persoons, A. M. McDonagh, M. D. Ward, J. A. McCleverty, Chem. Phys. Lett, 2003, **368**, 408; MP. Cifuentes, CE. Powell, JP. Morrall, AM. McDonagh, NT. Lucas, MG. Humphrey, M. Samoc, S. Houbrechts, I. Asselberghs, K. Clays, A. Persoons, T. Isoshima, J. Am. Chem. Soc, 2006, **128**, 10819; A. Wahab, M. Battacharya, S. Ghosh, A. G. Samuelson, P. K. Das, J. Phys. Chem B, 2008, **112**, 2842; N. Gauthier, G. Argouarch, F. Paul, L. Toupet, A. Ladjarafi, K. Costuas, J-F. Halet, M. Samoc, M. P. Cifuentes, C. T. Corkery, M. G. Humphrey, Chem. Eur. J, 2011, **17**, 5561.
58. B. Leiela, B. J. Coe, C. Koen, F. Stijn, V. Thierry, A. Inge, J. Am. Chem. Soc., 2008, **130**, 3286.
59. B. J. Coe, S. Houbrechts, J. Asselberghs, and A. Persoons, Angew. Chem. Int. Ed, 1999, **38**, 366.
60. G. J. Ashwell, J. Mater. Chem, 1999, **9**, 1991.
61. H. Sakaguchi, L. A. Gomez-Jahn, M. Prichard, T. L. Penner, D. G. Whitten, T. Nagamura, J. Phys. Chem, 1993, **97**, 1474; B. W. Chu, V. W. Yam, Inorg. Chem, 2001, **40**, 3324.
62. L. Boubekeur-Lecaque, B. J. Coe, J. A. Harris, M. Helliwell, I. Asselberghs, K. Clays, S. Foerier, T. Verbiest, Inorg. Chem, 2011, **50**, 12886.
63. R. H. Crabtree, A. J. Pearman, J. Organomet. Chem, 1977, **141**, 325.

64. T. Richardson, G. G. Roberts, M. E. C. Polywka, S. G. Davies. Thin. Solid. Films, 1988, **160**, 231.
65. A. K. Singh, D. S. Pandey, Q. Xu, P. Braunstein, Coord. Chem. Rev, 2014, 270–271, **31-56**, 270.
66. B. Linda, A. J. Godo, B. Zsolt, G. Eugenio, B. Peter, Eur. J. Inorg. Chem, 2013, 3090.
67. G. Winkhaus, H. Singer, J. Organomet. Chem, 1967, **7**, 487.
68. R. A. Zelonka, M.C.Baird, Can. J. Chem, 1972, **50**, 3063.
69. M. A. Bennett, A. K. Smith, J. Chem. Soc. Dalton. Trans, 1974, 233.
70. M. A. Bennett, T. W. Matheson, J. Organomet. Chem, 1979, **175**, 87.
71. M. Myahkostupov, F. N. Castellano, Inorg. Chem, 2011, **50**, 9714.
72. A. Abbotto, C. Coluccini, E. Dell'Orto, N. Manfredi, V. Trifiletti, M. M. Salamone, R. Ruffo, M. Acciarri, A. Colombo, C. Dragonetti, S. Ordanini, D. Roberto, A. Valorec, Dalton. Trans, 2012, **41**, 11731.
73. D. R. Baghurst, D. M. P. Mingos, J. Organomet. Chem, 1990, **384**, C57.
74. Y. Sun, M. L. Machala, F.N. Castellano, Inorg. Chim. Acta, 2010, **363**, 283.
75. T. Justus, R. Julie, G. Zacharias, S. Rosario, S. Kay, Eur. J. Inorg. Chem, 2013, 4558.
76. J. Grau, V. Noe, C. Ciudad, M. J. Prieto, M. Font-Bardia, T. Calvet, V. Moreno, J. Inorg. Biochem, 2012, **109**, 72.
77. B. S. Uppal, A. Zahid, P. I. P. Elliott, Eur. J. Inorg. Chem, 2013, 2571.
78. D. Carmona, J. Ferrer, I. M. Marzal, L. A. Oro, Gazzetta. Chimica. Italiana, 1994, **124**, 35.
79. C. A. Vock, C. Scolaro, A. D. Philips, R. Scopelliti, G. Sava, P. J. Dyson, J. Med. Chem, 2006, **49**, 5552.
80. K. J. Wallace, R. Daari, W. J. Belcher, L. O. Abouderbala, M. G. Boutelle, J. W. Steed, J. Organomet. Chem, 2003, **666**, 63.
81. A. A. Nazarov, C. G. Hartinger, P. J. Dyson, J. Organomet. Chem, 2014, **751**, 251.
82. A. V. Macatangay, J. F. Endicott, Inorg. Chem, 2000, **39**, 437.
83. S. Monika, L. Andreas, Polyhedron, 1986, **5**, 1217.
84. K. N. Kumar, G. Venkatachalam, R. Ramesh, Y. Liu, Polyhedron, 2008, **27**, 157.

85. P. Kumar, M. Yadav, A. Kumar. Singh, D. S. Pandey, Eur. J. Inorg. Chem, 2010, 704.
86. P. Barabotti, P. Diversi, G. Ingrosso, A. Lucherini, F. Marchetti, L. Sagramora, J. Chem. Soc. Dalton. Trans, 1990, 179.
87. R. Dussel, D. Pilette, P. H. Dixneuf, Organometallics, 1991, **10**, 3287.
88. M. A. Bennett, Acc. Chem. Res, 1997, **166**, 225.
89. A. Prades, E. Peris, M. Albrecht, Organometallics, 2011, **30**, 1162.
90. G. Suss-Fink, F. Khan, L. Juillerat-Jeanneret, P. J. Dyson, A. K. Renfrew, J. Clust. Sci, 2010, **21**, 313.
91. U. Kolle, R. Gorissen, A. Hornig, Inorg. Chim. Acta, 1994, **218**, 33.
92. A. Ramirez-Monroy, M. A. Paz-Sandoval, M. J. Ferguson, J. M. Stryker, Organometallics, 2007, **26**, 5010.
93. M. Gras, B. Therrien, G. Suss-Fink, P. Stepnicka, A. K. Renfrew, P. J. Dyson, J. Organomet. Chem, 2008, **693**, 3419.